Discovery and Profiling of a Selective and Efficacious Syk Inhibitor

ARTICLE *in* JOURNAL OF MEDICINAL CHEMISTRY · JANUARY 2015

Impact Factor: 5.45 · DOI: 10.1021/jm5018863 · Source: PubMed

10 AUTHORS, INCLUDING:

Maurice J Van Eis
Novartis
37 PUBLICATIONS **287** CITATIONS
SEE PROFILE

Eric Vangrevelinghe
Novartis
29 PUBLICATIONS **672** CITATIONS
SEE PROFILE

Reiner Aichholz
Novartis
45 PUBLICATIONS **702** CITATIONS
SEE PROFILE

Hans-Guenter Zerwes
Novartis
55 PUBLICATIONS **2,777** CITATIONS
SEE PROFILE

Journal of Medicinal Chemistry

Article

pubs.acs.org/jmc

Discovery and Profiling of a Selective and Efficacious Syk Inhibitor

Gebhard Thoma,*[,†] Alexander B. Smith,[†] Maurice J. van Eis,[†] Eric Vangrevelinghe,[†] Joachim Blanz,[‡] Reiner Aichholz,[‡] Amanda Littlewood-Evans,[§] Christian C. Lee,[∥] Hong Liu,[∥] and Hans-Günter Zerwes[§]

[†]Global Discovery Chemistry, [‡]Analytical Sciences & Imaging, [§]Autoimmunity, Transplantation and Inflammation Research, Novartis Institutes for Biomedical Research, 4056 Basel, Switzerland

[∥]Genomics Institute of the Novartis Research Foundation, 10675 John Jay Hopkins Drive, San Diego, California 92121, United States

ABSTRACT: We describe the discovery of selective and potent Syk inhibitor **11**, which exhibited favorable PK profiles in rat and dog and was found to be active in a collagen-induced arthritis model in rats. Compound **11** was selected for further profiling, but, unfortunately, in GLP toxicological studies it showed liver findings in rat and dog. Nevertheless, **11** could become a valuable tool compound to investigate the rich biology of Syk *in vitro* and *in vivo*.

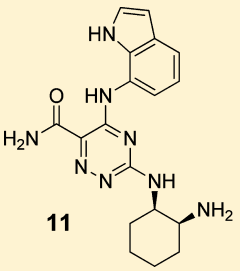

11

Syk (enzyme):	35 nM
Syk (cell):	99 nM
Syk (blood):	367 nM

INTRODUCTION

Spleen tyrosine kinase (Syk) is located in the cytoplasm of hematopoietic lineage cells except mature T cells. It plays a key role in mediating signal transduction via multiple receptors containing ITAM motifs (B-cell receptor in B-cells; Fc receptors in myeloid cells, basophils and mast cells; adhesion receptors; C-type lectin receptors). Following receptor stimulation, kinases of the src family phosphorylate tyrosine residues of the receptor intracellular ITAM domains, which serve as docking sites for the two SH2 domains of Syk. The kinase is recruited to the receptor and undergoes a conformational change, leading to full catalytic activity. Syk phosphorylates various substrates (such as BLNK in B cells, SLP76 in myeloid cells, PLCγ2a, Vav, PI3-kinase family members, Cbl) and becomes part of a multiprotein signaling complex, the signalosome, leading to the activation of downstream effector pathways such as PKC, MAPK, and NFκB.[1] Depending on the cell type and the trigger, effector functions such as proliferation, cytokine release, and oxidative burst are initiated. These are the basis of physiological responses associated with (auto)immune, inflammatory, or allergic reactions.

Blockade of the catalytic activity of Syk kinase is expected to abrogate these signaling pathways and to attenuate the biological responses. Thus, Syk is considered to be an attractive target for anti-inflammatory, antiallergic, and autoimmune diseases. In particular, prevention of activation of cells via immune complexes or antigen-triggered Fc receptor signaling and prevention of B cell receptor-mediated events are believed to have therapeutic potential.[2] To probe this hypothesis in animals and in clinical trials, the availability of selective, drug-like Syk inhibitors is highly desirable.

Compounds targeting Syk were tested in a battery of assays. Potency and kinase selectivity were assessed in enzymatic assays based on the Caliper microfluidic mobility shift technology. Cellular activity was measured in Ramos B-cells upon BCR stimulation with anti-IgM, which leads to phosphorylation of the adaptor protein BLNK (B cell linker protein), a direct Syk substrate. Inhibition of Syk in the presence of 90% human blood was monitored in monocytes following FcγR stimulation with an anti-CD32 antibody.[3] This leads to the phosphorylation of the adaptor protein SLP-76, which is also a direct substrate of Syk. To monitor cellular off-target inhibition (particularly Jak2), we used an assay measuring the IL3=dependent proliferation of mouse bone marrow cells.

Syk is an established target[3] first discovered in 1991.[4] Industry-wide efforts have been committed to identify selective antagonists,[5] but, to our knowledge, BIIB-057 **1**[6] (Figure 1) is the only selective Syk inhibitor that has been evaluated in clinical studies. However, a planned phase II trial in rheumatoid arthritis (RA) was withdrawn prior to patient enrollment.[7] The compound was potent in our enzymatic Syk assay (IC_{50} = 13 nM) and inhibited only 2 out of 77 additional kinases with IC_{50} values below 100 nM (ZAP70, 68 nM; PKCα, 90 nM; Table 1). Substantial activity was observed in the cellular Syk assay (IC_{50} = 178 nM). In human blood monocytes stimulated by activating CD32 in the presence of blood, Syk activity was inhibited with an IC_{50} value of ~1 μM. However, in both automated[8] and manual patch clamp assays,[9] **1** significantly affected hERG channel activity with IC_{50} values around 10 μM.

Recently, Gilead disclosed the structure of GS-9973 **2**, which is being evaluated in cancer clinical trials.[10] Their compound was described as a highly potent and selective Syk inhibitor. However, in our assays, **2** showed only modest activity, particularly in the presence of blood (IC_{50} > 19 μM, Table 1). It is important to note that **2** considerably affected bone marrow cell proliferation, which cannot be explained by Syk inhibition (Table 1).

In a previous communication, we reported a series of napthyridinone and pyridopyrimidinone Syk inhibitors with

Received: December 5, 2014
Published: January 29, 2015

DOI: 10.1021/jm5018863
J. Med. Chem. 2015, 58, 1950−1963

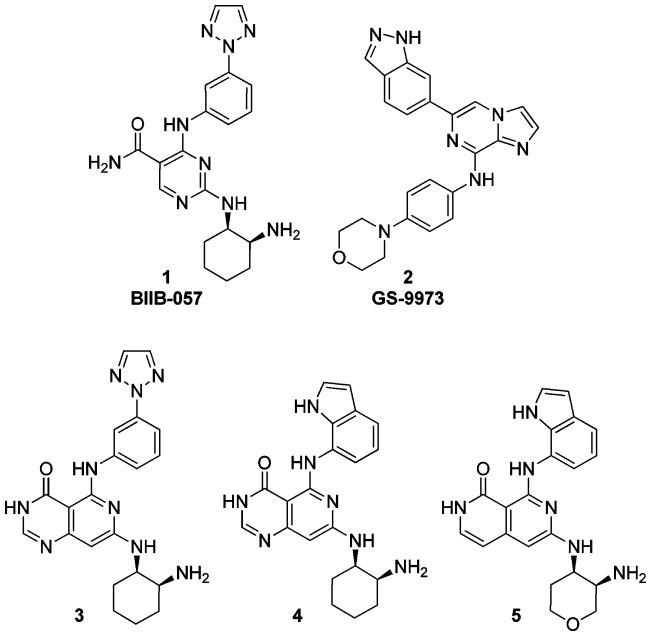

Figure 1. Structures of clinical compounds **1** and **2** as well as structures of reference compounds **3**–**5**.

bicyclic cores sharing the binding mode of compound **1**.[11] Initial compounds such as **3** containing substituted anilines displayed poor kinase selectivity and moderate cellular activity (IC_{50} = 778 nM, Table 1). In contrast, replacement of aniline with a 7-aminoindole substituent led to compounds such as **4** and **5** with acceptable kinase selectivity, good cellular activity (IC_{50} < 100 nM), high potency in the presence of blood (IC_{50} < 500 nM), and little or no hERG channel inhibition (Table 1). Unfortunately, we failed to improve the poor PK properties of these compounds, and, consequently, this series was abandoned. In efforts to overcome these PK liabilities, we investigated monocyclic analogues of **1** based on pyridine (**6** and **7**), pyrazine (**8** and **9**), triazine (**10**–**12**), and pyrimidine cores (**13**).

Here, we describe discovery and profiling of the potent, highly selective, and orally bioavailable Syk inhibitor **11**, which shares the binding mode of **1**, **3**, **4** and **5**.

CHEMISTRY

Pyridine derivative **6** was prepared from building block **14** (Scheme 1). The reaction with aniline **15** led to **16**. Compound

Scheme 1. Synthesis of Compound 6[a]

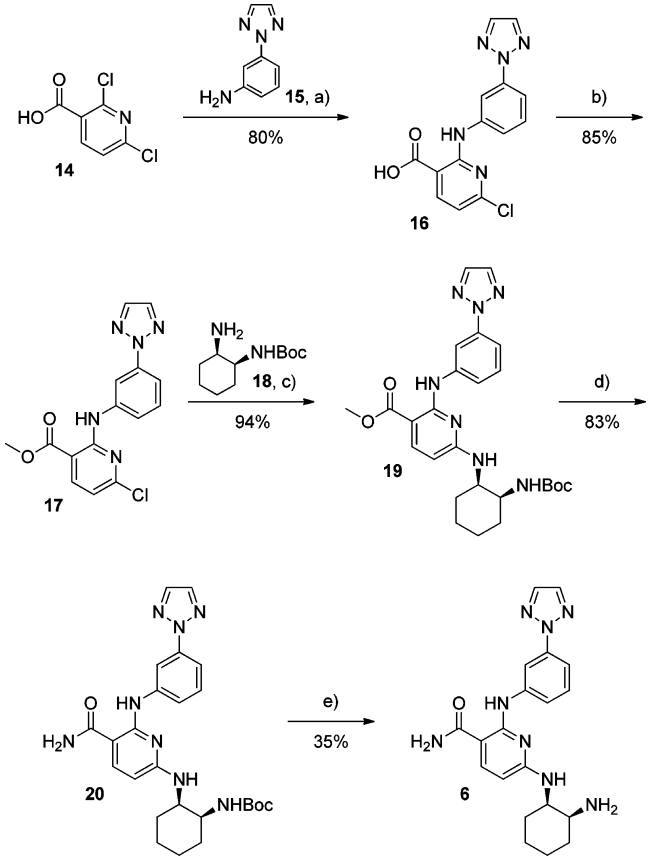

[a]Reagents and conditions: (a) (1) **15**, LiHMDS, THF, 1 h, −78 °C, (2) add **14**, −78 → 25 °C, 1 h; (b) (1) CDI, DMF, 16 h, 25 °C, (2) add MeOH, 0.5 h, 25 °C; (c) **18**, DIPEA, NMP, 16 h, 120 °C; (d) (1) LiOH, H_2O, dioxane, 2 h, 100 °C, (2) COMU, DIPEA, DMF, NH_4OH, 1 h, 25 °C; (e) TFA, CH_2Cl_2, 1 h, 25 °C.

15 was treated with an excess of LiHMDS (3 equiv) prior to the addition of acid **14** to obtain the desired regioisomer **16** in

Table 1. Key *in Vitro* Data

compound	Syk[a] (enzyme)	kinase[b] selectivity	BM cell prolif.	Syk[a] (cell)	Syk[a] (blood)	hERG[a] Q-patch	hERG[c] man. patch
1	13 ± 4	2 (77)	5853	178 ± 8	952 ± 70	8600	42% at 10 μM 72% at 30 μM
2	377 ± 90	0 (58)	582	878 ± 88	19 416 ± 1474	n.d.	n.d.
3	5 ± 2	9 (36)	249	778 ± 132	n.d.	n.d.	n.d.
4	4 ± 0.6	3 (55)	3411	90 ± 15	307 ± 123	>30 000	n.d.
5	22 ± 1	1 (55)	3515	55 ± 2	433 ± 159	24 900	n.d.
6	19 ± 8	2 (59)	2601	445 ± 75	n.d.	8500	n.d.
7	165 ± 45	0 (59)	>10 000	438 ± 34	n.d.	>30 000	n.d.
8	1 ± 0.2	12 (67)	2110	69 ± 15	1788 ± 98	10 000	n.d.
9	5 ± 1	4 (69)	5267	30 ± 2	302 ± 57	8100	13% at 3 μM 50% at 10 μM
10	5 ± 0.6	6 (64)	811	104 ± 29	274 ± 48	3700	n.d.
11	35 ± 4	0 (69)	9020	99 ± 7	367 ± 27	25 900, >30 000	0% at 10 μM 12% at 30 μM
12	1[d]	6 (58)	5270	14 ± 1	177 ± 53	3700	n.d.
13	94 ± 2	0 (67)	>10 000	170 ± 54	782 ± 372	>30 000	n.d.

[a]IC_{50} in nanomolar; $n \geq 3$ for Syk enzyme, cell, and blood assays (SEM shown). [b]Number of kinases with IC_{50} < 100 nM in addition to Syk (number of kinases tested). [c]Inhibition at indicated concentration; three independent measurements for each concentration. [d]Tested once.

DOI: 10.1021/jm5018863
J. Med. Chem. 2015, 58, 1950−1963

good yield. Compound **16** was transformed into methyl ester **17**. The Boc-protected diaminocyclohexane **18** was introduced, giving **19**, which was converted into amide **20**. Removal of the protecting group afforded compound **6**.

Compound **7** was accessible from building block **21** (Scheme 2). The Boc-protected diaminocyclohexane **18** was introduced

Scheme 2. Synthesis of Compound 7[a]

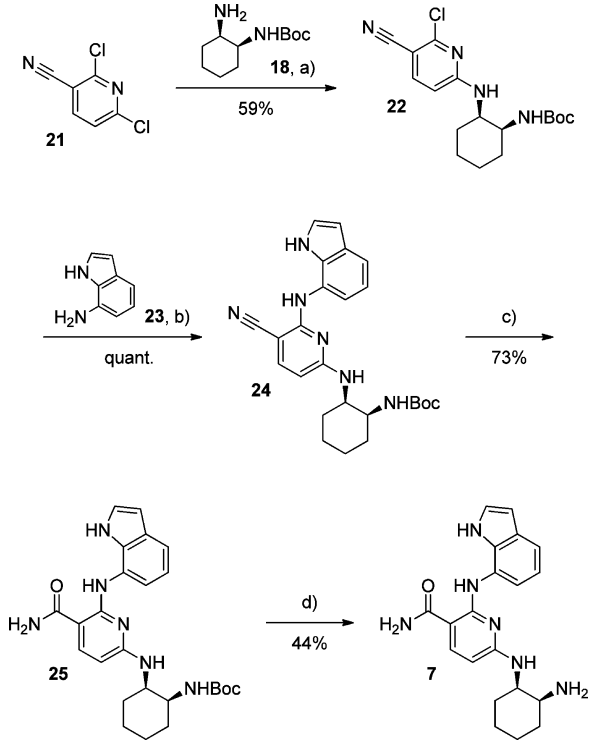

[a]Reagents and conditions: (a) **18**, NMP, NEt_3, 16 h, 75 °C; (b) **23**, $Pd(OAc)_2$, Xantphos, K_2CO_3, dioxane, 1.5 h, 150 °C; (c) H_2O_2, NaOH, DMSO, EtOH, 3 h, 25 °C; (d) HCl, CH_2Cl_2, 2 h, 0 → 25 °C.

to give **22**. Palladium-catalyzed coupling with aminoindole **23** led to **24**, which was transformed into amide **25**. Deprotection afforded compound **7**.

Pyrazine **8** was obtained from building block **26**, which was reacted with the Boc-protected diaminocyclohexane **18** to give **27** (Scheme 3). The regioisomer of **27** was also isolated (19%). Introduction of aniline **15** led to **28**, which was transformed into amide **29**. Deprotection afforded compound **8**.

Indole derivative **9** was obtained from building block **30**, which was reacted with the Boc-protected diaminocyclohexane **18** to give **31** (Scheme 4). Introduction of aminoindole **23** led to **32**, which was transformed into amide **33**. Deprotection led to compound **9**.

Triazine **10** was prepared from building block **34**, which was reacted with aniline **15** to give **35** (Scheme 5). Compound **35** was transformed into amide **36**. Oxidation of **36** with *m*-CPBA led to the formation of a mixture of sulfoxide and sulfone, which was treated with the Boc-protected diaminocyclohexane **18** to give **37**. Deprotected afforded compound **10**.

Indole derivative **11** was also prepared from building block **34** (Scheme 6). The introduction of 7-aminoindole **23** led to **38**. The indole was protected to give **39**, which was transformed into amide **40**. The sulfur atom of compound **40** was oxidized, leading to a mixture of sulfoxide and sulfone. Susequent treatment with Boc-protected diaminocyclohexane

Scheme 3. Synthesis of Compound 8[a]

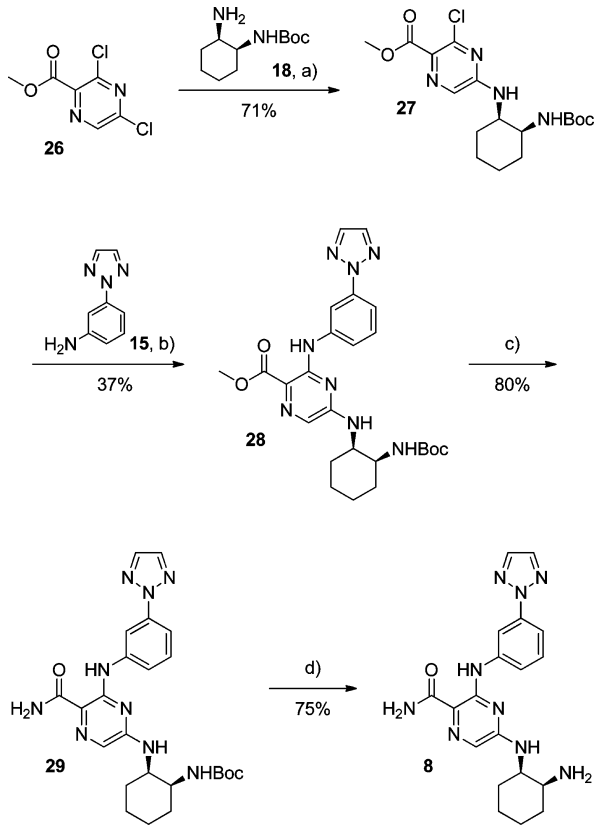

[a]Reagents and conditions: (a) **18**, DMF, NEt_3, 16 h, 0 → 25 °C; (b) **15**, $Pd(OAc)_2$, Xantphos, K_2CO_3, dioxane, 16 h, 90 °C; (c) (1) LiOH, H_2O, dioxane, 2 h, 25 °C, (2) COMU, DIPEA, DMF, NH_4OH, 0.5 h, 25 °C; (d) HCl, CH_2Cl_2, MeOH, 16 h, 25 °C.

18 gave **41**. Deprotection furnished compound **11**. The deprotection had to be carefully monitored because of the formation of side products, which were difficult to separate (probably dimerization of the indole due to the acidic reaction conditions). Compound **12** was prepared following analogous procedures but using 4-aminoindole instead of 7-aminoindole (see Experimental Section).

Pyrimidine **13** was prepared from building block **42**, which was reacted with aminoindole **23** to give **43** (Scheme 7). Introduction of benzyloxycarbonyl-protected diaminocyclohexane **44** led to **45**, which was deprotected to afford compound **13**. The benzyloxycarbonyl-protected building block **44** was used to avoid acidic deprotection conditions, which led to side product formation in the synthesis of compound **11**.

RESULTS AND DISCUSSION

Compounds **6**–**13** were broadly assessed and compared to competitor compound **1** (Table 1). In the enzymatic Syk assay, triazolyl-anilines **1**, **6**, **8**, and **10** (IC_{50} values of 13, 19, 1, and 5 nM, respectively) were generally found to be more potent than corresponding 7-aminoindoles **13**, **7**, **9**, and **11** (IC_{50} values of 94, 165, 5, and 35 nM, respectively). However, in the cellular Syk assay, compound pairs with the same core structure showed similar potency (pyrimidines **1** and **13**, 178 and 170 nM; pyridines **6** and **7**, 445 and 438 nM; pyrazines **8** and **9**, 69 and 30 nM; triazines **10** and **11**, 104 and 99 nM). With the exception of pyridines **6** and **7**, all new compounds **8**–**13** were at least equipotent to **1**. As we had observed previously for

DOI: 10.1021/jm5018863
J. Med. Chem. 2015, 58, 1950−1963

Scheme 4. Synthesis of Compound 9[a]

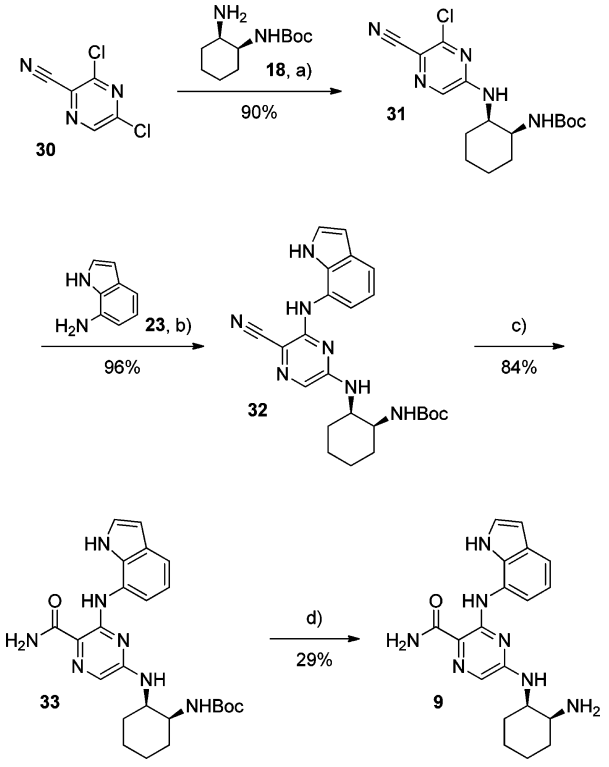

[a]Reagents and conditions: (a) **18**, DMF, NEt_3, 16 h, 0 → 25 °C; (b) **23**, $Pd(OAc)_2$, Xantphos, K_2CO_3, dioxane, 16 h, 90 °C; (c) H_2O_2, NaOH, DMSO, EtOH, 2 h, 0 → 25 °C; (d) HCl, CH_2Cl_2, MeOH, 16 h, 25 °C.

Scheme 5. Synthesis of Compound 10[a]

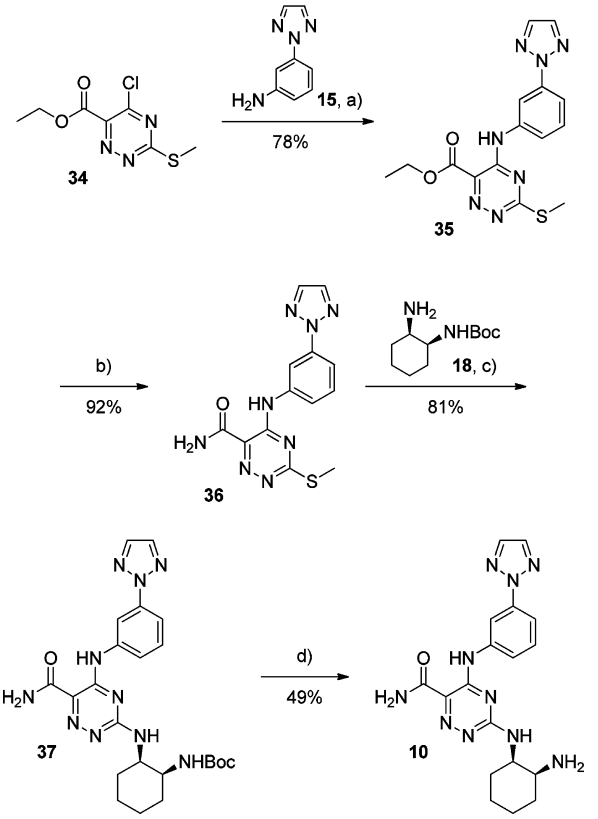

[a]Reagents and conditions: (a) **15**, NMP, 0.5 h, 0 → 25 °C; (b) NH_3 (7 M) in MeOH, 2 h, 25 °C; (c) (1) *m*-CPBA, DMF, 2 h, 0 → 45 °C, (2) **18**, NEt_3, 2 h, 25 → 65 °C; (d) TFA, CH_2Cl_2, 1 h, 25 °C.

related bicyclic compounds **3**–**5**[11] (Table 1), 7-aminoindoles **13**, **7**, **9**, and **11** were found to be more selective in our enzymatic kinase panel than corresponding triazolyl-anilines **1**, **6**, **8**, and **10**. The inferior selectivity of the triazolyl-anilines compared to that of the 7-aminoindoles was confirmed by more pronounced effects in the bone marrow cell proliferation assay, which is independent of Syk (Table 1). 4-Aminoindole **12** was found to be the most potent compound, with IC_{50} values of 1 and 14 nM in the enzymatic and cellular assays, respectively. Unfortunately, **12** showed limited selectivity, inhibiting 6 out of 58 kinases with IC_{50} values below 100 nM, but it did not significantly affect bone marrow cell proliferation (IC_{50} > 5 μM). We previously had observed the reduced kinase selectivity of 4-aminoindole derivatives with bicyclic cores sharing the binding mode of the compounds discussed here.[11]

To understand the superior kinase selectivity of the 7-aminoindoles, we compared the high-resolution X-ray costructures of compounds **10** and **11** bound to Syk catalytic domain.[12] Both triazolyl-aniline **10** and corresponding indole **11** form two strong hydrogen bonds with the hinge sequence of Syk (E449, A451; Figure 2). Both the aniline of **10** and the indole of **11** are sandwiched between the side chain of L377 and P455 located at the proximal P-loop and downstream hinge regions, respectively. However, the orientation of the aromatic substituents differs. The N-linked triazole of **10** is oriented toward the diaminocyclohexane, whereas the five-membered ring of the indole of **11** is directed toward the downstream hinge region of Syk. Overall, the bioactive (bound) conformation of aniline **10** is more compact compared to that of **11**. The indole of **11** can form an additional H-bond with A451. However, this H-bond is most likely weak, as the carbonyl oxygen of A451 and the nitrogen of the indole are not optimally positioned. The weakness of the hydrogen bond is supported by the slightly inferior activity of the 7-aminoindoles in the biochemical assay. As we did not attempt to co-crystallize our compounds with other kinases, the rationale for the superior selectivity of the 7-aminoindoles remained elusive.

Pyrimidine **1** and pyridine **6** showed superior kinase selectivity compared to that of pyrazine **8** and triazine **10**. In contrast to **1** and **6**, compounds **10** and **8** can form an intramolecular H-bond between the amide NH and the triazine core, which is expected to reduce the rotation of the amide out of the plane of the aromatic ring (Figure 3A). This assumption was supported by DFT/B3LYP calculations in the gas phase,[12] which indicated a more pronounced distortion of the amide for **1** compared to **10** with dihedral angles of 16° and 2°, obtained for the respective optimized geometries (Figure 3B). As compound **3** with a perfectly planar bicyclic pyridopyrimidinone core, which shares the binding mode of compounds **1**, **6**, **8**, and **10**, also showed limited kinase selectivity (Table 1),[11] we speculated that a distortion of the hinge-binding amide motif improves the kinase selectivity of compounds with this binding mode. However, when we analyzed the structures of pyrimidine **1** and triazine **10** bound to Syk catalytic domain, we learned that the bound conformations superimposed almost perfectly and showed very small distortions of the amide with similar dihedral angles of ~8° and ~4° for **1** and **10**, respectively.

Pyrazines **8** and **9** as well as triazines **10** and **11**, which form an intramolecular H-bond (flat core), were more potent but

DOI: 10.1021/jm5018863
J. Med. Chem. 2015, 58, 1950–1963

Scheme 6. Synthesis of Compounds 11 and 12[a]

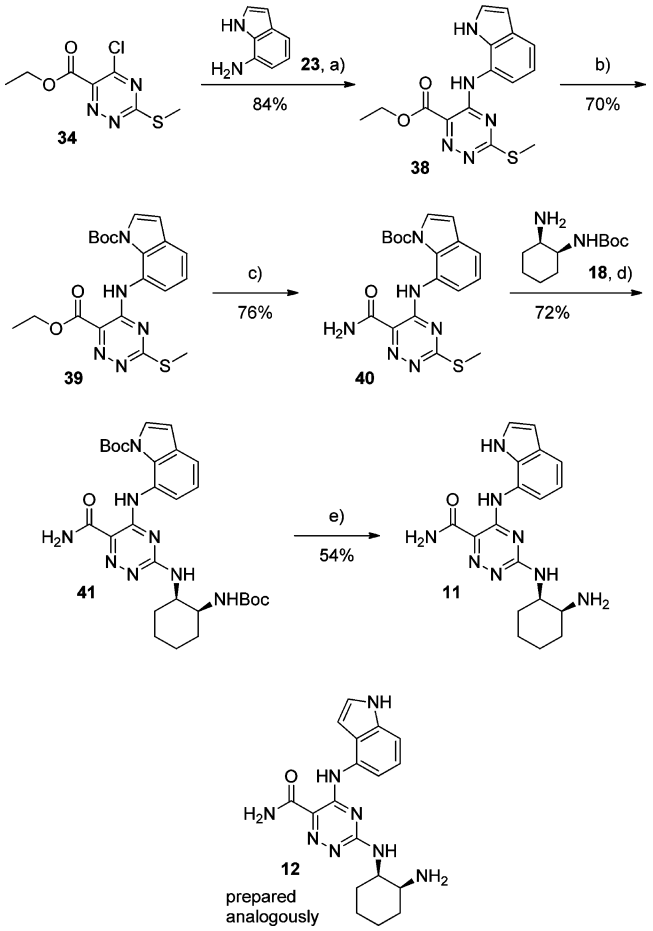

[a]Reagents and conditions: (a) **23**, NMP, 0.25 h, 25 °C; (b) DMAP, $(Boc)_2O$, THF, 0.5 h, 0 → 25 °C; (c) NH_3 (7 M) in MeOH, 0.75 h, 25 °C; (d) (1) *m*-CPBA, DMF, 0.75 h, 0 °C, (2) **18**, NEt_3, 0.25 h, 65 °C; (e) TFA, H_2O, CH_2Cl_2, 17.5 h, 0 → 25 °C.

Scheme 7. Synthesis of Compound 13[a]

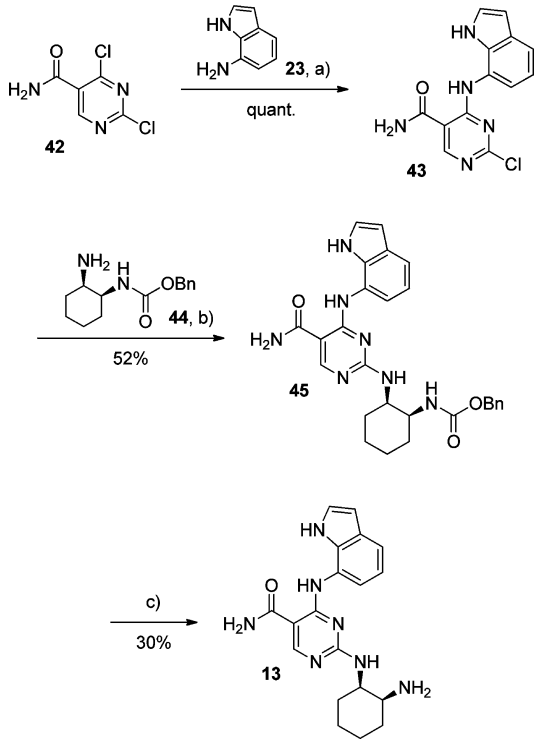

[a]Reagents and conditions: (a) **22**, THF, NEt_3, 16 h, 25 °C; (b) **44**, DMF, NEt_3, 3 h, 110 °C; (c) Pd/C, H_2, MeOH, 3.5 h, 25 °C.

less selective than corresponding pyridines **6** and **7** or pyrimidines **1** and **13**, which do not form an intramolecular H-bond (Table 1). Thus, compounds **9** and **11** combining a 7-aminoindole substituent (inducing selectivity) and a flat core (inducing potency) were considered to be the most promising.

Compounds **8**, **9**, **10**, **11**, **12**, and **13** were tested for Syk inhibition in whole blood monocytes (IC_{50} values of 1788, 302, 274, 367, 177, and 782 nM, respectively) and, with the exception of **8**, were found to be superior to **1** (IC_{50} = 952 nM). Interestingly, compared to 7-aminoindole **11**, corresponding 4-aminoindole **13** was only 2-fold more potent in the blood assay despite its clearly superior potencies in both the enzymatic and cellular assays (35-fold and 7-fold, respectively). Inhibition of the hERG channel was assessed in an automated patch clamp assay (Q-patch, Table 1).[8] 7-Aminoindoles **13**, **7**, and **11** showed reduced effects (IC_{50} > 20 μM) compared to their triazolyl-aniline analogues, **1**, **6**, and **10** (IC_{50} < 10 μM). Pyrazines **8** and **9** showed similar IC_{50} values (~10 μM). 4-Aminoindole **12** significantly inhibited hERG channel activity with an IC_{50} value of 3.7 μM. Compounds **9** and **11** were also tested in a manual patch clamp assay.[9] Pyrazine **9** considerably inhibited hERG channel activity (50% at 10 μM), whereas triazine **11** did not show any inhibition at 10 μM and only 12% inhibition at 30 μM and, thus, differentiated favorably from compound **1**.

Compounds **9** and **11** showed favorable PK properties in rat (Table 2). Medium clearance (CL) and high volume of distribution (V_{SS}) led to long mean residence times (MRT). Both exposure (AUC) and oral bioavailability (BAV) were acceptable. Slow absorption led to flat PK curves, avoiding high peak concentrations (Figure 4). In dogs, compound **11** also showed good exposure, acceptable oral bioavailability, and a long MRT (Table 2). Corresponding 4-aminoindole **12** showed very limited exposure, higher clearance, and a shorter MRT.[13] Due to the poor PK properties, hERG channel inhibition, and limited selectivity, the slightly more potent compound **12** was not further considered (2-fold more potent than **9** and **11** in the most relevant whole blood assay, Table 1).

Compound **11** was selected for further profiling. For a broader exploration of the kinase selectivity, the binding of **11** to a panel of 451 kinases was assessed (Figure 5).[14] Only 14 of the kinases demonstrated remarkable binding affinity to **11**, and K_d values were determined. Compound **11** was found to bind most strongly to Syk (K_d = 0.64 nM), exhibiting 20-fold selectivity over Pak7, 25-fold selectivity over Pak4, and ≥100-fold selectivity over the remaining kinases. The K_d for Zap70, which is the closest analogue of Syk, was 65 nM, resulting in a selectivity factor of 100. In the biochemical Caliper assays, we observed only a 7-fold selectivity over Zap70 (Table 3). However, in a cellular assay interrogating Zap70 activity (anti-CD3-induced Zap70-dependent phosphorylation of SLP76 in Jurkat cells), compound **11** was found to be 25-fold less potent than in a similar assay interrogating Syk activity (anti-IgM-induced BLNK phosphorylation; Table 3). Compound **1** showed only 10-fold selectivity in this most relevant cellular

DOI: 10.1021/jm5018863
J. Med. Chem. 2015, 58, 1950−1963

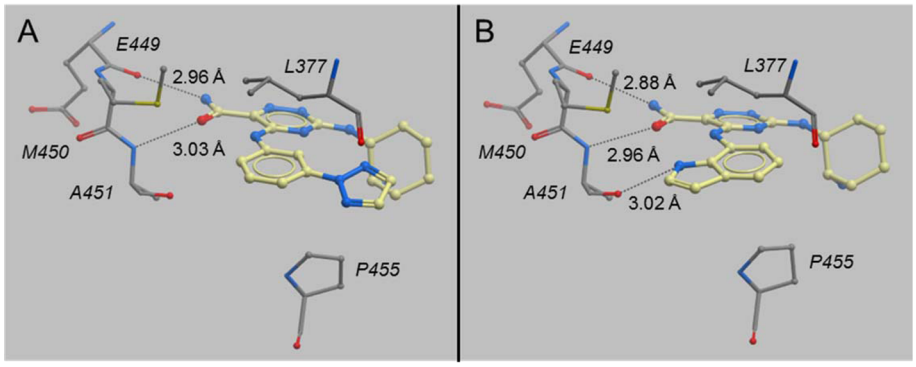

Figure 2. Crystal structures of triazines **10** (A) and **11** (B) bound to the kinase domain of Syk.

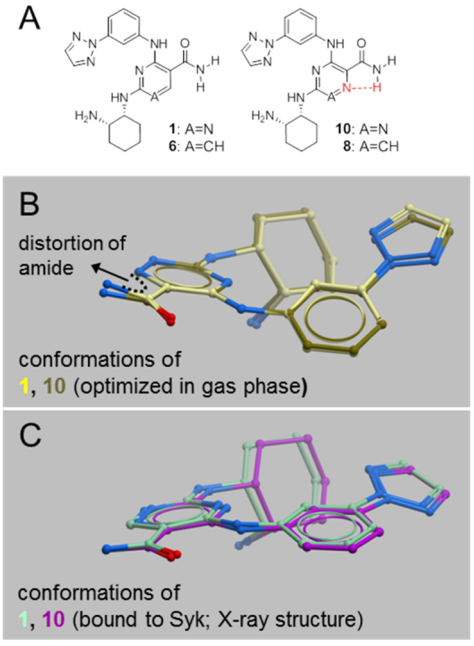

Figure 3. (A) Compounds **10** and **8** can form an intramolecular H-bond; compounds **1** and **6** cannot. Thus, an increased distortion of the amide is expected for **1** and **6**. (B) DFT/B3LYP calculations in the gas phase[12] indicate a more pronounced distortion of the amide for **1** compared to that for **10**, with dihedral angles of 16° and 2°, measured for the respective optimized geometries. (C) The conformations of compounds **1** and **10** bound to the Syk catalytic domain superimpose almost perfectly and show very small distortions of the amide with similar dihedral angles of ~8° and ~4° for **1** and **10**, respectively. For simplicity, the amino acids of the protein are omitted.

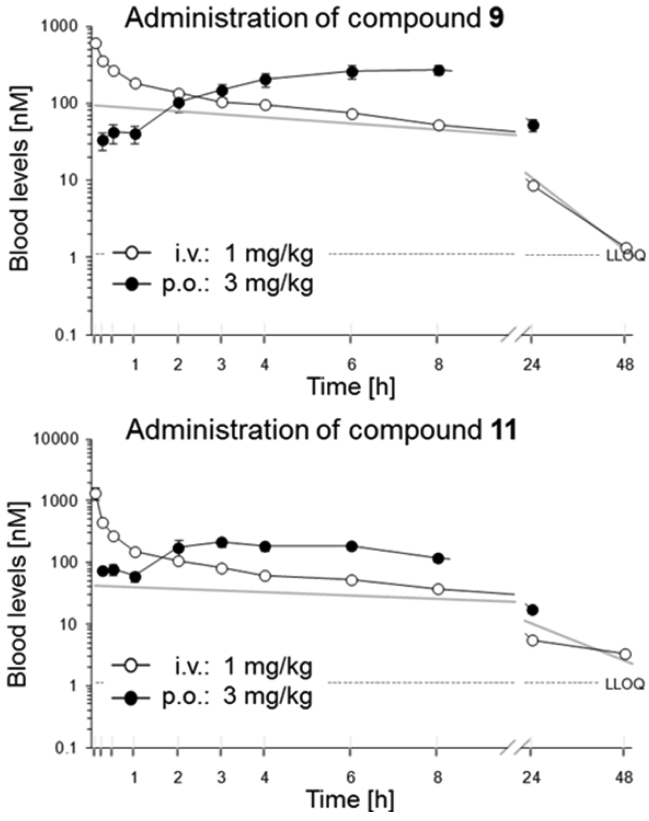

Figure 4. PK curves for **9** and **11** following i.v. and p.o. dosing in rat.

Table 2. PK Data on Compounds 9, 11, and 12

parameter	9	11		12
species	rat[a]	rat[a]	dog[b]	rat[a]
CL (mL min^{-1} kg^{-1})	28	31	11	83
V_{SS} (L/kg)	12.3	16.4	6.8	10.3
MRT (h)	7.2	8.7	8.4	2.1
AUC iv[c] (nM h)	1610	1459	3414	522
AUC po[c] (nM h)	1523	877	1836	19
BAV (%)	95	60	54	4
C_{max}[c] (nM)	108	80	139	4

[a]Cassette dosing in Sprague–Dawley rats; i.v. 1 mg/kg, NMP/PEG200 (3:7); p.o. 3 mg/kg, CMC/water/Tween (0.5:99:0.5). [b]One-in-one dosing in Beagle dogs; i.v. 0.1 mg/kg, NMP/PEG200 (3:7); p.o. 0.3 mg/kg, MC/water (0.5:99.5). [c]Dose normalized.

assay. Overall, compound **11** exhibited a very promising kinase selectivity profile, warranting further experiments.

We established a rat PK/PD model in which compound **11** was administered to Lewis rats (Figure 4). Blood samples were taken at different times postdosing for PK determinations as well as assessment of inhibition of Syk-dependent signaling events. For this, the extent of SLP76 phosphorylation in monocytes in response to stimulation by anti-CD32 was quantified. A representative experiment is shown in Figure 6A. A dose of 22 mg/kg of **11** led to 90, 85, and 45% inhibition after 2, 4, and 24 h postadministration, respectively. Blood concentrations were 900, 1100, and 300 nM, respectively. Analysis of individual samples from several experiments involving different doses (30–3 mg/kg) and time points (2, 4, 24 h) indicated a dose- and exposure-dependent inhibition of the PD response *ex vivo* (FcgR-induced P-SLP76 in peripheral

DOI: 10.1021/jm5018863
J. Med. Chem. 2015, 58, 1950–1963

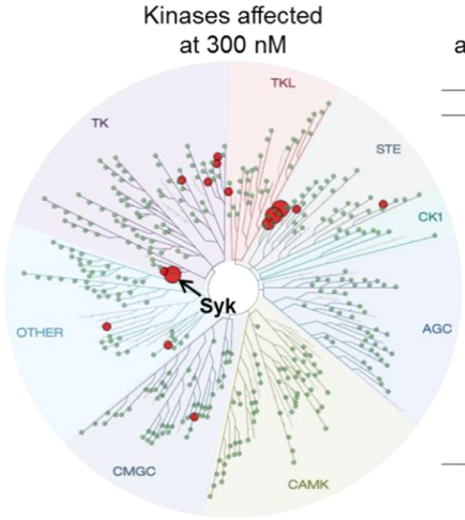

K_d values on affected kinases

Kinase	K_d [nM]
AXL	71
BUB1	240
GCN2	150
IRAK1	67
JAK2	53
MAP3K2	140
MERTK	150
PAK4	17
PAK6	110
PAK7	12
ROS1	120
SLK	380
SYK	0.64
ZAP70	65

Figure 5. Kinase selectivity profile of compound **11**. In addition to Syk, only 13 out of 451 kinases were affected at a concentration of 300 nM. For these kinases, K_d values were determined.

Table 3. Selectivity of Compound 11 over Zap70

assay [nM]	**1**	**11**
Syk (enzyme)	13 ± 4	35 ± 4
Syk (K_d)	n.d.	0.64
Syk (cell)	178 ± 8	99 ± 7
Zap70 (enzyme)	76 ± 13	251 ± 23
Zap70 (K_d)	n.d.	65
Zap70 (cell)	1805 ± 305	2526 ± 493

blood monocytes) with blood IC_{50} levels of 189 nM (Figure 6B).

Efficacy of **11** was demonstrated *in vivo* in a rat collagen-induced arthritis model in which the compound dosing was started when rats developed paw swelling (day 15) subsequent to immunization (day 0) and boost (day 7) with porcine collagen.[15] In this therapeutic model, compound **11** showed rapid and sustained reversal of paw swelling at 10 and 30 mg/kg p.o. q.d. and inhibition of swelling at 3 mg/kg p.o. q.d. with slow onset but significant inhibition vs placebo (Figure 7A). The treated animals displayed higher body weight gain compared to that in vehicle-treated animals due to reduced joint swelling and good tolerability of compound **11** (Figure 7B). The reversal of joint swelling was also reflected in improved histology (reduced inflammation and cartilage and proteoglycan loss; Figure 7C). Peak compound concentrations in the blood of treated animals were 126, 866, and 2891 nM for the doses of 3, 10, and 30 mg/kg, respectively (Figure 7D). It is worth mentioning that a statistically significant reduction in joint swelling (3 mg/kg dose) was observed at exposure levels below the IC_{50} value of 189 nM determined for **11** in the PK/PD model.

Because of its favorable profile, compound **11** was investigated in toxicology studies in rats and dogs. Unfortunately, in 4 week GLP studies, we observed liver findings such as single necrosis of hepatocytes, bile plugs, and portal inflammation. Furthermore, in the GLP *in vitro* hERG assay, compound **11** showed an IC_{50} value of 5 μM, which was unexpected considering the non-GLP data (Table 1). However, in a dog telemetry study, no prolongation of the QT interval was observed. Compound **11** was nonetheless abandoned

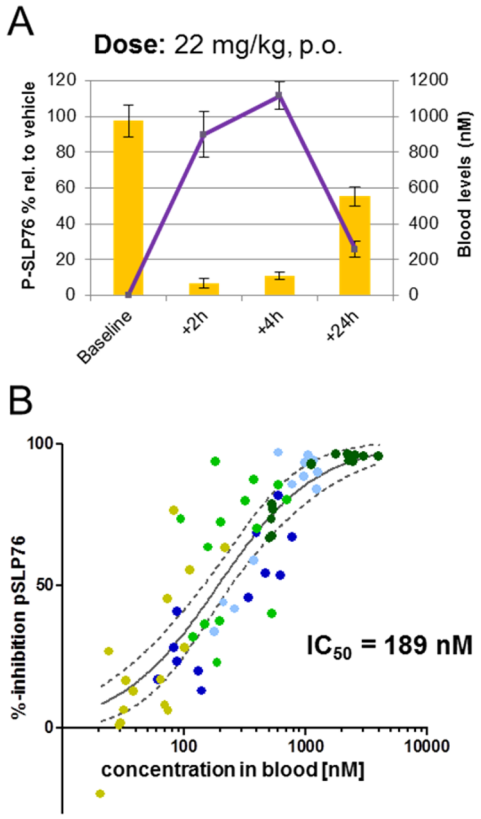

Figure 6. PK/PD experiments with compound **11**. (A) Single-dose treatment of Lewis rats followed by *ex vivo* assessment of blood compound levels (PK) and FcgR-induced P-SLP76 in peripheral blood monocytes (PD). (B) The IC_{50} value was determined by PK/PD analysis of individual samples from several experiments involving several doses (30−3 mg/kg) as well as several time points (2, 4, 24 h). The colors indicate data from distinct dosing groups (dark green, 30 mg/kg; light blue, 22 mg/kg; light green and dark blue, 10 mg/kg; yellow, 3 mg/kg).

mainly because of an insufficient therapeutic index for autoimmune indications.

As Syk expression is limited to hematopoietic lineage cells,[1] we attributed the liver findings to the chemical structure of **11** but not to its mode of action. Studies of the metabolism of **11** *in vitro* (liver microsomes) and *in vivo* (rat) did not indicate the presence of reactive metabolites. However, experiments with radiolabeled **11** in hepatocytes pointed to covalent adduct formation. Furthermore, incubation of **11** with hepatocytes afforded cysteine conjugate **46** (Figure 8A), which possibly originated from a reactive metabolite trapped by glutathione or cysteine. To the best of our knowledge, the formation of a cysteine adduct such as **46** is unprecedented. Metabolite **46** (0.9 μg) was isolated from incubation of parent compound **11** with monkey liver slices. The structure was assigned by NMR based on the following observations (Figure 8B): (a) The spin system H-4, H-5, H-6 was observed by TOCSY (total correlation spectroscopy), indicating that there was no additional substitution compared to **11**. (b) A proton of the indole nitrogen (N-1) was not observed. (c) The signal for H-4 was shifted to 8.31 ppm (7.44 ppm in **11**, Figure 8C), which is in line with a deshielding effect of the carbonyl function at C-3. (d) A single proton at the nitrogen (N-18) of the cysteine was detected, and the chemical shift of 4.12 ppm for H-19 indicated an N-linked cysteine. Additional evidence came from MS

DOI: 10.1021/jm5018863
J. Med. Chem. 2015, 58, 1950−1963

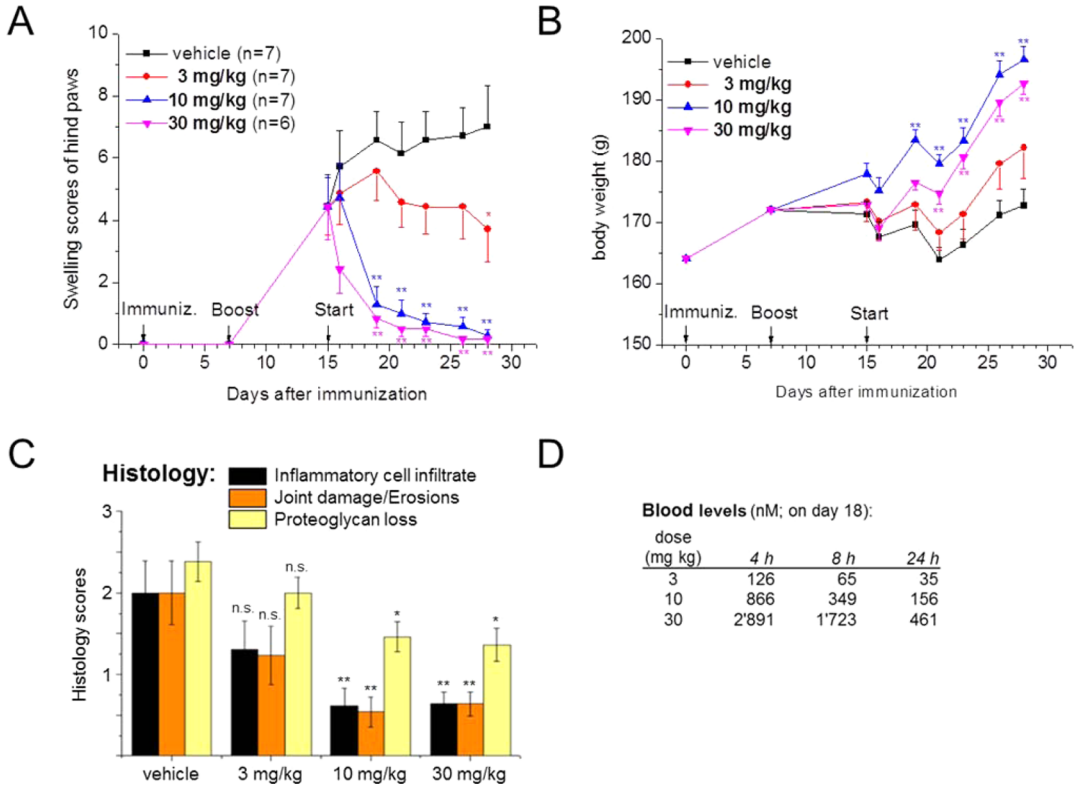

Figure 7. Inhibition of collagen-induced arthritis in female Lewis rats by compound **11**. (A) Rats were immunized on day 1 with collagen and boosted after 7 days. Joint swelling developed in hind paws. Rats with swollen joints were randomized to treatment groups. Compound **11** was administered once daily at the indicated doses. (B) Body weight of treated and untreated rats. (C) Histology scores for inflammation and bone and cartilage damage in hind paws at termination of the experiment on day 28. (D) Blood levels of compound **11** for all doses were determined on day 18 (third day of treatment) at the indicated time points.

experiments (Figure 8D). Collision-induced dissociation of the protonated molecular ion of **46** (m/z = 500) resulted in the loss of CO_2 (m/z = 456) followed by the loss of hydrogen sulfide (m/z = 422). The loss of hydrogen sulfide can occur only if the cysteine is linked to the indole via nitrogen but not if it is linked via sulfur. The elemental formula of **46** and the fragment ions was supported by accurate mass measurements. The metabolic pathway leading to **46**, the structure of the primary metabolite, and the contribution of this metabolite to the observed liver findings remain elusive.

■ CONCLUSIONS

We have described the discovery and characterization of the efficacious and selective Syk inhibitor **11**. Unfortunately, compound **11** could not be advanced to clinical trials because of liver findings in toxicology studies, limiting the therapeutic index. However, we believe that compound **11** is a good tool compound to study the biology of Syk *in vitro* and *in vivo*.

■ EXPERIMENTAL SECTION

General. Reagents, solvents, and heterocyclic building blocks (**14**, **21**, **26**, **30**, **34**, and **42**) were purchased from commercial sources and used without further purification. All reactions were carried out under an atmosphere of argon. High-resolution LC/ESI-MS data were recorded using a Thermo Scientific LTQ Orbitrap XL mass spectrometer with an electrospray ionization source and a Shimadzu Nexera liquid chromatograph equipped with a diode array detector. The NMR spectra were obtained using a 400 MHz spectrometer. All ^{1}H NMR spectra are reported in δ units (ppm) and were recorded in DMSO-d_6 or CD_3OD and referenced to the solvent peaks. Liquid chromatography was performed on Acquity UPLC/MS systems (Waters, Milford, MA) equipped with a binary solvent manager, a sample manager, a column manager, a photodiode array detector (PDA), and a Waters ZQ2000 MS detector. Acquity UPLC columns (Waters, Milford, MA) with dimensions of 2.1 × 50 mm and packed with high-strength silica (HSS) T3 particles of 1.8 μ diameter and 100 Å pore size were used. The columns were housed at constant 60 °C inside the column manager with a tolerance band of 0.1 °C. The flow was 1 mL/min. The mobile phase consisted of (A) water + 0.05% formic acid and (B) acetonitrile + 0.04% formic acid. The runtime was 2 min. The following gradient was used: from A/B 95:5 → 2:98 within 1.40 min; A/B 2:98 for 0.4 min; from A/B 2:98 → 95:5 within 0.1 min; A/B 95:5 for 0.1 min. UV absorption was monitored at λ = 210−450 nM. The MS detector was operated in continuously positive/negative ESI alternating mode with full scan from 120 to 1200 Da in 0.3 s. Mass spectra were acquired and stored in centroid mode. MS-based confirmation of molecular weight was based on the formation of the pseudomolecular ions $[M + H]^+$ in positive mode and $[M - H]^-$ in negative mode. All test compounds reported in this article had a purity >95%.

Structure Elucidation of 46. NMR spectra (^{1}H, ^{13}C, 2D ROESY (rotating frame nuclear Overhauser effect), HSQC (heteronuclear single quantum coherence), and HMBC (heteronuclear multiple bond correlation) were measured on a Bruker AVANCE III spectrometer (600 MHz proton frequency) equipped with a 1.7 mm ^{1}H{^{13}C,^{15}N} Bruker BioSpin TCI MicroCryoProbe. ^{1}H and ^{13}C shifts were referenced internally to the solvent signals at 2.50 and 39.5 ppm, respectively. Each metabolite sample was dissolved in about 40 μL of DMSO-d_6 and transferred to a 1.7 mm NMR tube. MS investigations were performed on a LTQ XL Orbitrap (linear quadrupole 2D ion trap/Orbitrap, Thermo Scientific, CA) mass spectrometer equipped with a captive spray ionization (CSI) source (Michrom BioResources, Auburn, CA) operating in positive mode electrospray ionization (ESI). The resolution was set to 30 000 in full scan and 15 000 in MS(n)

DOI: 10.1021/jm5018863
J. Med. Chem. 2015, 58, 1950−1963

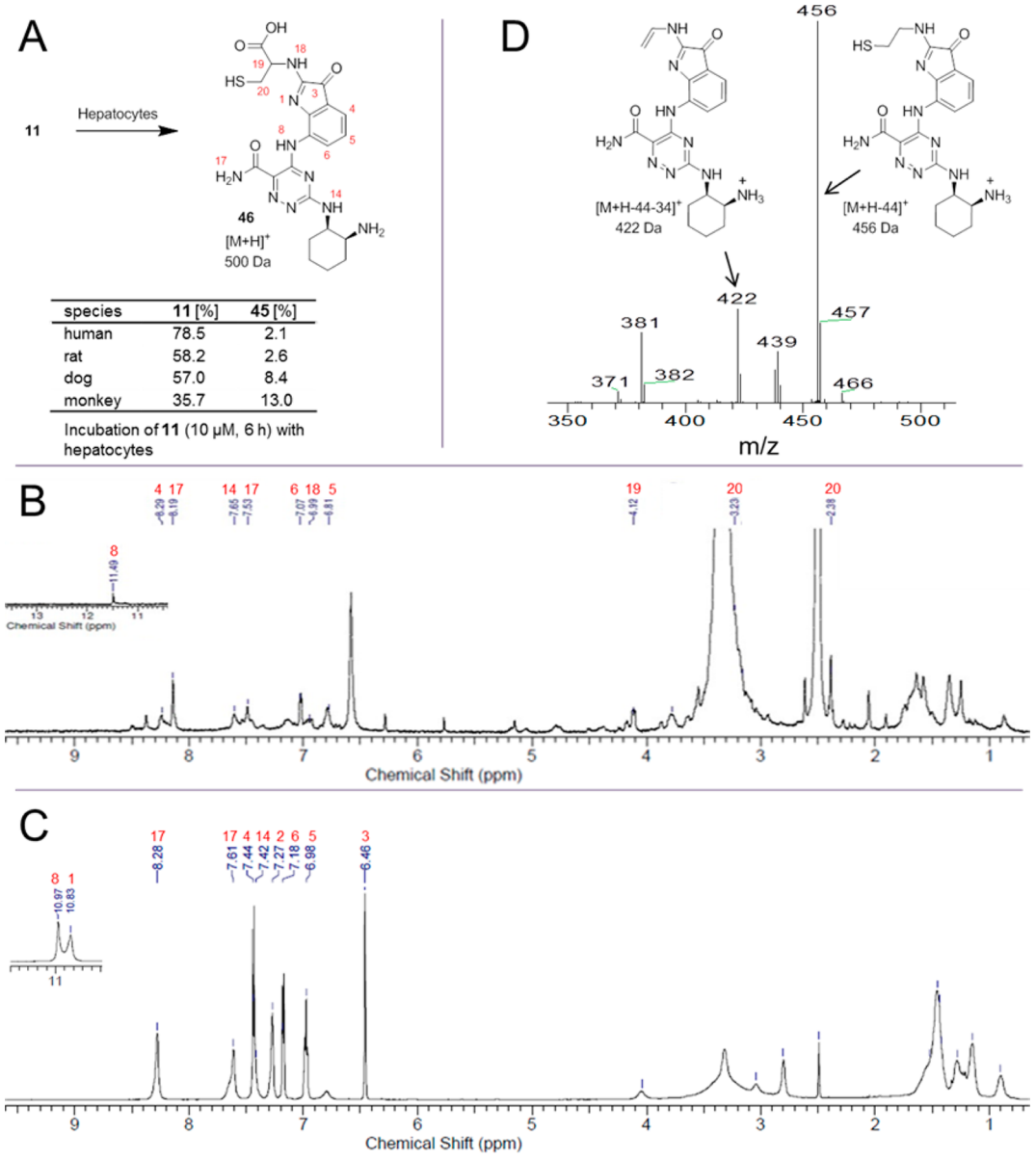

Figure 8. Metabolite **46**. (A) Formation in hepatocytes from different species. (B) ^{1}H NMR spectrum of **46** and assignment of key signals (0.9 μg, DMSO-d_6). (C) ^{1}H NMR spectrum of **11** and assignment of key signals (DMSO-d_6). Additional signals and broadening of signals due to existence of different rotamers. (D) Collision-induced fragmentation of the protonated molecular ion of **46**.

mode. The omnipresent polysiloxane background ion $[C_2H_6SiO]_6$ with m/z 445.12003 was used as external lock mass.

16. LiHMDS (21.7 mL of 1 M solution in THF, 21.7 mmol) was added at −78 °C to a solution of **15** (1193 mg, 7.45 mmol) in THF (15 mL), and the mixture was stirred for 1 h. A solution of **14** (1300 mg, 6.77 mmol) in THF (5 mL) was added at −78 °C, and the mixture warmed to 25 °C and stirred for 1 h. The mixture was poured into ice-cold 2 N HCl, extracted with CH_2Cl_2, and dried with Na_2SO_4, and the solvent was removed. The residue was crystallized from cyclohexane/ether to yield **16** as a light brown solid (1700 mg, 79%). UPLC retention time 1.09 min. ^{1}H NMR (DMSO-d_6): δ 13.9 (1H, s), 10.78 (1H, m), 8.53 (1H, m), 8.28 (1H, d), 8.15 (2H, s), 7.73 (1H, m), 7.64 (1H, m), 7.54 (1H, t), 7.00 (1H, d). ES/ESI 316 $[M + H]^+$.

17. To a solution of **16** (1700 mg, 5.38 mmol) in DMF (10 mL) was added CDI (1528 mg, 9.45 mmol), and the mixture was stirred for 16 h at 25 °C. Methanol (10 mL) was added within 10 min, and stirring was continued for 30 min. The mixture was poured into water, and the precipitate was filtered off. Compound **17** (1650 mg, 92%) was isolated as a brown solid. UPLC retention time 1.32 min. ^{1}H NMR (DMSO-d_6): δ 10.33 (1H, m), 8.54 (m, 1 H), 8.29 (1H, d), 8.14 (2H, s), 7.74 (m, 1 H), 7.62 (1H, m), 7.54 (1H, t), 7.02 (1H, d), 3.91 (3H, s). ES/ESI 330 $[M + H]^+$.

19. A mixture of **17** (500 mg, 1.516 mmol), **18** (487 mg, 2.275 mmol), and DIPEA (588 mg, 4.55 mmol) in NMP (5 mL) was stirred for 16 h at 120 °C. The mixture was cooled to 25 °C, poured into water, and extracted with ethyl acetate, and the organic phase was dried with Na_2SO_4. The solvent was removed, and the residue was purified by chromatography (ethyl acetate/cyclohexane gradient) to yield **19** (720 mg, 93%) as a yellow oil. UPLC retention time 1.42 min. ^{1}H NMR (DMSO-d_6): δ 10.65 (1H, m), 8.84 (1H, m), 8.12 (2H, s), 7.82 (1H, m), 7.63 (1H, m), 7.47 (2H, m), 7.12 (1H, m), 6.42 (1H, m), 6.11 (1H, d), 4.31 (1H, m), 3.83 (1H, m), 3.80 (3H, s), 1.78−1.05 (8H, m), 1.28 (9H, s). ES/ESI 508 $[M + H]^+$.

20. A mixture of **19** (710 mg, 1.399 mmol), LiOH·H_2O (293 mg, 7 mmol), dioxane (4 mL), and water (1 mL) was stirred for 2 h at 100 °C. The mixture was cooled to 25 °C, water (50 mL) was added, the pH was adjusted to 1 with 4 N HCl, and it was extracted with CH_2Cl_2. The organic phase was dried with Na_2SO_4, and the solvent was removed to give 571 mg of the acid of **19**, which was used without

DOI: 10.1021/jm5018863
J. Med. Chem. 2015, 58, 1950−1963

further purification in the next step. UPLC retention time 1.21 min. ES/ESI 494 $[M + H]^+$. A mixture of the acid (250 mg, 0.507 mmol), DIPEA (72 mg, 0.557 mmol), and COMU (239 mg, 0.557 mmol) in DMF (3 mL) was stirred at 25 °C for 10 min, NH_4OH (10 mmol) was added, and stirring was continued for 1 h. The mixture was poured into aqueous $NaHCO_3$ and extracted with ethyl acetate, and the organic phase dried with Na_2SO_4. The solvent was removed, and the residue was purified by chromatography (ethyl acetate/cyclohexane gradient) to yield **20** (250 mg, 83% over 2 steps) as a yellow oil. UPLC retention time 1.15 min. ^1H NMR (DMSO-d_6): δ 12.05 (1H, s), 8.76 (1H, m), 8.10 (2H, s), 7.81 (1H, m), 7.56 (1H, m), 7.43 (2H, m), 6.73 (1H, m), 6.41 (1H, m), 6.03 (1H, d), 4.31 (1H, m), 3.82 (1H, m), 1.80−1.08 (8H, m), 1.28 (9H, s). ES/ESI 493 $[M + H]^+$.

6. A mixture of **20** (250 mg, 0.508 mmol) and TFA (1157 mg, 10 mmol) in CH_2Cl_2 (2 mL) was stirred at 25 °C for 1 h. The solvent was removed, and the residue was purified by preparative HPLC. Product containing fractions were combined and passed through an Isolute SCX-2 column to yield the free base of **6** (70 mg, 35%) as a yellow solid. UPLC retention time 0.65 min. ^1H NMR (DMSO-d_6): δ 12.05 (1H, s), 8.75 (1H, m), 8.10 (2H, s), 7.80 (1H, d), 7.65 (1H, m), 7.55 (1H, m), 7.43 (2H, m), 7.05 (1H, m), 6.73 (1H, m), 6.41 (1H, m), 6.07 (1H, d), 4.13 (1H, m), 3.07 (1H, m), 1.70−1.20 (8H, m). HR-MS $[M + H]^+$ calcd, 393.21458; found, 393.21469.

22. A mixture of **21** (1000 mg, 5.78 mmol), **18** (1363 mg, 6.36 mmol), and NEt_3 (702 mg, 6.94 mmol) in NMP (10 mL) was stirred at 75 °C for 16 h. The mixture was poured into ice water, the pH was adjusted to 1 with concentrated HCl, and the precipitate was collected. Chromatography (ethyl acetate/cyclohexane gradient) gave **22** (1200 mg, 59%) as a colorless solid. UPLC retention time 1.17 min. ^1H NMR (DMSO-d_6): δ 7.70 (1H, m), 7.46 (1H, m), 6.61 (1H, m), 6.27 (1H, m), 4.10 (1H, m), 3.77 (1H, m), 1.72−1.25 (8H, m), 1.33 (9H, s). ES/ESI 351 $[M + H]^+$.

25. A mixture of **22** (500 mg, 1.425 mmol), **22** (226 mg, 1.71 mmol), $Pd(OAc)_2$ (19.2 mg, 0.086 mmol), Xantphos (99 mg, 0.172 mmol), and K_2CO_3 (2954 mg, 21.38 mmol) in dioxane (16 mL) was heated at 150 °C for 1.5 h. The mixture was diluted with ethyl acetate (40 mL) and washed with 0.1 N HCl, saturated $NaHCO_3$ solution, and brine. The organic phase was dried with Na_2SO_4, and the solvent was removed to give crude **24** (890 mg), which was used without purification for the next step. UPLC retention time 1.24 min. ES/ESI 447 $[M + H]^+$. A mixture of **24** (636 mg, 1.425 mmol), 4 N NaOH (1.78 mL, 7.13 mmol), H_2O_2 (0.728 mL 30% solution), ethanol (8 mL), and DMSO (4 mL) was stirred at 25 °C for 3 h. The mixture was poured into water and extracted with saturated $NaHCO_3$ solution and brine. The organic phase was dried with Na_2SO_4, the solvent was removed, and the residue was purified by chromatography (ethyl acetate/cyclohexane gradient) to yield **25** (500 mg, 73% over 2 steps) as a light brown solid. UPLC retention time 1.11 min. ^1H NMR (DMSO-d_6): δ 11.40 (1H, s), 10.50 (1H, s), 7.79 (1H, d), 7.55 (1H, m), 7.47 (1H, d), 7.23 (3H, m), 6.91 (1H, t), 6.50 (1H, m), 6.42 (1H, m), 6.37 (1H, m), 5.91 (1H, d), 3.82 (1H, m), 3.67 (1H, m), 1.65−1.15 (8H, m), 1.33 (9H, s). ES/ESI 465 $[M + H]^+$.

7. At 0 °C, 4 N HCl in dioxane (5.27 mL, 21.1 mmol) was added to a solution of **25** (490 mg, 1.055 mmol) and CH_2Cl_2 (30 mL). The ice bath was removed, and the mixture was stirred for 2 h at 25 °C. Ethyl acetate was added, and the mixture was washed with $NaHCO_3$ solution and brine. The organic phase was dried with Na_2SO_4, and the solvent was removed. The residue was purified by chromatography (ethyl acetate/methanol/NH_3 gradient) to give 7 (169 mg, 44%) as a colorless solid. UPLC retention time 0.61 min. ^1H NMR (DMSO-d_6) (100 °C; rotamers, not all NH signals visible): δ 10.70 (1H, s), 10.18 (1H, s), 7.81 (1H, d), 7.42 (2H, m), 7.28 (1H, d), 7.20 (2H, m), 6.93 (1H, t), 6.42 (1H, m), 6.01 (1H, d), 3.82 (1H, m), 3.19 (1H, m), 1.72−1.15 (8H, m). HR-MS $[M + H]^+$ calcd, 365.20844; found, 365.20850.

27. At 0 °C, a solution of **18** (2950 mg, 13.76 mmol) in DMF (5 mL) was added to a solution of **26** (2590 mg, 12.51 mmol) and NEt_3 (1267 mg, 12.51 mmol) in DMF (20 mL). The ice bath was removed, and the mixture was stirred for 16 h at 25 °C. The mixture was diluted with ethyl acetate and washed with water and brine. The organic phase was dried with Na_2SO_4, and the solvent was removed. The residue was purified by chromatography (ethyl acetate/cyclohexane gradient) to give the regioisomer of **27** (950 mg, 19%) as a yellow solid and **27** (3460 mg, 71%) as a colorless solid. Regioisomer of **27**: UPLC retention time 1.21 min. ^1H NMR DMSO-d_6 δ = 8.28 (1H, d), 7.89 (1H, s), 6.93 (1H, d), 4.27 (1H, m), 3.84 (3H, s), 3.81 (1H, m), 1.68−1.15 (8H, m), 1.31 (9H, s). ES/ESI 385 $[M + H]^+$. **27**: UPLC retention time 1.03 min. ^1H NMR (DMSO-d_6): δ 7.98 (1H, s), 7.90 (1H, d), 6.70 (1H, d), 4.15 (1H, m), 3.77 (3H, s), 3.75 (1H, m), 1.70−1.15 (8H, m), 1.32 (9H, s). ES/ESI 385 $[M + H]^+$.

28. A mixture of **27** (300 mg, 0.780 mmol), **15** (187 mg, 1.169 mmol), $Pd(OAc)_2$ (1.8 mg, 0.008 mmol), Xantphos (9.0 mg, 0.016 mmol), K_2CO_3 (1077 mg, 7.89 mmol), and dioxane (2 mL) was heated at 90 °C for 16 h. The mixture was diluted with ethyl acetate and washed with 0.1 N HCl, $NaHCO_3$ solution, and brine. The organic phase was dried with Na_2SO_4, and the solvent was removed. The residue was purified by chromatography (ethyl acetate/cyclohexane gradient) to give **28** (150 mg, 37%) as a colorless solid. UPLC retention time 1.23 min. ^1H NMR (DMSO-d_6): δ 10.60 (1H, s), 8.82 (1H, m), 8.11 (2H, s), 7.72 (1H, m), 7.68 (1H, d), 7.56 (1H, s), 7.51 (1H, t), 7.41 (1H, m), 6.60 (1H, d), 4.25 (1H, m), 3.90 (1H, m), 3.82 (3H, s), 1.79−1.05 (8H, m), 1.31 (9H, s). ES/ESI 509 $[M + H]^+$.

29. A mixture of **27** (150 mg, 0.295 mmol), $LiOH·H_2O$ (49.5 mg, 1.18 mmol), water (0.5 mL), and dioxane (1 mL) was stirred at 25 °C for 2 h. Ethyl acetate was added, and the mixture was washed with 0.1 N HCl and brine. The organic phase was dried with Na_2SO_4, and the solvent was removed to give the acid of **27**, which was used without purification for the next step. UPLC retention time 1.16 min. ES/ESI 495 $[M + H]^+$. DIPEA (36 mg, 0.279 mmol) and COMU (131 mg, 0.307 mmol) were added to a solution of the acid of **27** (138 mg) in DMF (2 mL), and the mixture was stirred at 25 °C for 5 min. NH_3 (0.24 mL 25% aqueous solution, 6.14 mmol) and DIPEA (36 mg, 0.279 mmol) were added, and the mixture was stirred at 25 °C for 30 min. The mixture was diluted with ethyl acetate and washed with saturated $NaHCO_3$ solution and brine. The organic phase was dried with Na_2SO_4, and the solvent was removed to give **29** (117 mg, 80%), which was used without purification for the next step. UPLC retention time 1.17 min. ^1H NMR (DMSO-d_6): δ 11.75 (1H, s), 8.80 (1H, m), 8.10 (2H, s), 7.77 (m, 1 H), 7.62 (1H, d), 7.50−7.35 (4H, m), 7.30 (1H, m), 6.53 (1H, m), 4.30 (1H, m), 3.92 (1H, m), 1.78−1.05 (8H, m), 1.29 (9H, s). ES/ESI 494 $[M + H]^+$.

8. A mixture of **29** (117 mg, 0.237 mmol), concentrated HCl (4.74 mmol), CH_2Cl_2 (10 mL), and methanol (1 mL) was stirred at 25 °C for 16 h. Ethyl acetate (20 mL) was added, and the mixture was washed with saturated $NaHCO_3$ solution. The organic phase was evaporated to a smaller volume, and **8** was precipitated by the addition of cyclohexane (74 mg of a light brown solid, 75%). UPLC retention time 0.74 min. ^1H NMR (DMSO-d_6): δ 11.75 (1H, s), 8.88 (1H, m), 8.12 (2H, s), 7.79 (1H, m), 7.62 (1H, d), 7.55 (1H, s), 7.54 (1H, m), 7.48 (1H, t), 7.35 (2H, m), 4.21 (1H, m), 3.84 (1H, m), 3.20 (2H, m), 1.78−1.25 (8H, m). HR-MS $[M + H]^+$ calcd, 394.20983; found, 394.20960.

31. At 0 °C, **17** (739 mg) in DMF (2 mL) was added to a solution of **30** (500 mg) and NEt_3 (0.401 mL, 2.87 mmol) in DMF (5 mL), and the mixture was stirred for 16 h at 25 °C. The mixture was diluted with ethyl acetate (50 mL) and washed with water (50 mL). The aqueous phase was extracted with ethyl acetate (30 mL), the combined organic phases were washed with brine and dried over Na_2SO_4, and the solvent was removed. Chromatography on silica (gradient cyclohexane/ethyl acetate) gave **31** (905 mg, 90%) as a colorless solid. UPLC retention time 1.13 min. ^1H NMR (DMSO-d_6): δ 8.36 (1H, m), 8.02 (1H, s), 6.79 (1H, d), 4.17 (1H, m), 3.77 (1H, m), 1.70−1.25 (8H, m), 1.32 (9H, s). ES/ESI 352 $[M + H]^+$.

32. To **31** (300 mg) in dioxane (2 mL) were added under argon **23** (135 mg), K_2CO_3 (1178 mg), $Pd(OAc)_2$ (1.91 mg), and Xantphos (9.9 mg,). The mixture was stirred for 16 h at 90 °C. The mixture was diluted with ethyl acetate (20 mL) and washed with HCl (0.1 N; 30 mL). The aqueous phase was extracted with ethyl acetate (20 mL), the combined organic phases were washed with bicarbonate solution and brine and dried over Na_2SO_4, and the solvent was removed.

DOI: 10.1021/jm5018863
J. Med. Chem. 2015, 58, 1950−1963

Chromatography on silica (gradient cyclohexane/ethyl acetate) gave **32** (368 mg, 96%). UPLC retention time 1.19 min. ES/ESI 448 $[M + H]^+$.

33. To **32** (368 mg) in DMSO (2 mL) and EtOH (4 mL) was added at 0 °C 4 N NaOH (1.03 mL) and H_2O_2 (0.382 mL). After stirring for 2 h at 25 °C, the mixture was partitioned between water and ethyl acetate (30 mL each). The organic phase was washed with bicarbonate solution and brine and dried over Na_2SO_4, and the solvent was removed to give crude **32** (320 mg), which was used without further purification in the next step. UPLC retention time 1.18 min. ^{1}H NMR (DMSO-d_6): δ 11.05 (1H, s), 10.70 (1H, m), 7.67 (1H, m), 7.38 (2H, m), 7.30 (1H, d), 7.23 (1H, t), 7.20 (2H, m), 6.50 (1H, m), 6.43 (1H, m), 3.75 (2H, m), 1.65−1.05 (8H, m), 1.31 (9H, s). ES/ESI 466 $[M + H]^+$.

9. To **33** (320 mg) in CH_2Cl_2 (20 mL) and MeOH (4 mL) was added 4 N HCl (3.44 mL), and the mixture was stirred for 16 h at 25 °C. The mixture was diluted with CH_2Cl_2 (50 mL), washed with bicarbonate solution and brine, and dried with Na_2SO_4, and the solvent was removed. Chromatography using a KP-NH column (gradient MeOH/ethyl acetate) gave **9** (74 mg, 29%) as a yellow solid. UPLC retention time 0.65 min. ^{1}H NMR (DMSO-d_6): δ 11.04 (1H, s), 10.71 (1H, s), 7.67 (1H, m), 7.42 (1H, s), 7.32 (1H, d), 7.28 (1H, d), 7.24 (1H, m), 7.22 (1H, m), 7.18 (1H, m), 6.93 (1H, t), 6.44 (1H, m),3.65 (1H, m), 2.87 (1H, m), 1.55−1.03 (8H, m). HR-MS $[M + H]^+$ calcd, 366.20368; found, 366.20353.

35. Compound **15** (360 mg, 2.245 mmol) was added to a solution of **34** (500 mg, 2.140 mmol) in NMP (2.5 mL) at 0 °C, the cooling bath was removed, and the mixture was stirred for 30 min at 25 °C. The suspension was diluted with methanol (3.5 mL), and the precipitate was filtered off, washed with diethyl ether, and dried to give **35** (608 mg, 78%) as a beige solid. UPLC retention time 1.12 min. ^{1}H NMR (DMSO-d_6): δ 10.40 (1H, s), 8.73 (1H, m), 8.15 (2H, s), 7.87 (1H, m), 7.58 (2H, m), 4.46 (2H, q), 2.60 (3H, s), 1.39 (3H, t). ES/ESI 360 $[M + H]^+$.

36. A suspension of **35** (300 mg, 0.823 mmol) in NH_3/methanol (3 mL 7N solution) was stirred at 25 °C for 2 h. The mixture was poured into ice water, and the precipitate was filtered off, washed with water, and dried to give **36** (254 mg, 92%) as a beige solid. UPLC retention time 0.95 min. ^{1}H NMR (DMSO-d_6): δ 11.90 (1H, s), 8.80 (2H, m), 8.15 (3H, m), 7.83 (1H, d), 7.60 (1H, t), 7.55 (1H, d), 2.61 (3H, s). ES/ESI 329 $[M + H]^+$.

37. To a suspension of **36** (250 mg, 0.746 mmol) in DMF (2.5 mL) was added at 0 °C *m*-CPBA (334 mg, 1.492 mmol), the ice bath was removed, and the mixture was stirred for 2 h at 45 °C. To the yellow suspension were added at 25 °C NEt_3 (385 mg, 3.81 mmol) and **18** (196 mg, 0.913 mmol). The mixture was stirred for 2 h at 65 °C. The mixture was concentrated and purified by preparative HPLC to give **37** (323 mg, 81%) as a beige solid. UPLC retention time 1.03 min. ES/ESI 495 $[M + H]^+$.

10. A solution of **37** (323 mg, 0.655 mmol) and TFA (1.5 mL, 19.5 mmol) in CH_2Cl_2 (2 mL) was stirred at 25 °C for 1 h. The solvent was removed, and the residue was purified by preparative HPLC. Product containing fractions were combined, the solvent was removed, and the residue was dissolved in CH_2Cl_2. The organic phase was washed with 1 N NaOH and dried over Na_2SO_4, and the solvent was removed to give the free base **10** (130 mg, 49%). UPLC retention time 0.64 min. ^{1}H NMR (DMSO-d_6): δ 11.70 (1H, s), 8.92 (1H, s), 8.38 (1H, s), 8.12 (2H, s), 7.75 (3H, m), 7.54 (1H, t), 7.42 (1H, m), 3.97 (1H, m), 3.08 (1H, m), 1.73−1.22 (8H, m). HR-MS $[M + H]^+$ calcd, 395.20508; found, 395.20486.

38. Compound **23** (283 mg, 2.140 mmol) was added to a solution of **34** (500 mg, 2.140 mmol) in NMP (2 mL), and the mixture was stirred at 25 °C for 15 min. The mixture was added to water, and the precipitate was collected and dried to give compound **38** (660 mg, 84%) as a beige solid. UPLC retention time 1.07 min. ^{1}H NMR (DMSO-d_6): δ 10.81 (1H, s), 10.00 (1H, s), 7.53 (1H, d), 7.34 (1H, t), 7.11 (1H, d), 7.03 (1H, t), 6.49 (1H, m), 4.49 (2H, q), 2.01 (3H, s), 1.41 (3H, t). ES/ESI 330 $[M + H]^+$.

39. To a suspension of **38** (660 mg, 1.803 mmol) and DMAP (22.5 mg, 0.180 mmol) in THF (4 mL) was added at 0 °C a solution of $(Boc)_2O$ (437 mmg, 1.984 mmol) in THF (3 mL). The mixture was stirred at 25 °C for 30 min. The solvent was removed, and the residue was purified by chromatography on silica (gradient cyclohexane/ethyl acetate) to give compound **39** (555 mg, 70%) as a yellow solid. UPLC retention time 1.28 min. ^{1}H NMR (DMSO-d_6): δ 10.50 (1H, s), 7.67 (1H, d), 7.61 (1H, d), 7.44 (1H, d), 7.32 (1H, t), 6.77 (1H, d), 4.48 (2H, q), 2.09 (3H, s), 1.40 (3H, t), 1.38 (9H, s). ES/ESI 430 $[M + H]^+$.

40. A mixture of **39** (260 mg, 0.593 mmol) and NH_3 (2 mL of a 7 molar solution in methanol) was stirred at 25 °C for 45 min. The mixture was added to ice water, and the precipitate was collected and dried to give compound **40** (183 mg, 76%). UPLC retention time 1.09 min. ^{1}H NMR (DMSO-d_6): δ 11.50 (1H, s), 8.67 (1H, s), 8.05 (1H, s), 7.68 (1H, d), 7.61 (1H, d), 7.36 (1H, d), 7.31 (1H, t), 6.77 (1H, d), 2.09 (3H, s), 1.32 (9H, s). ES/ESI 401 $[M + H]^+$.

41. To a solution of **40** (180 mg, 0.445 mmol) in DMF (2 mL) was added *m*-CPBA (199 mg, 0.890 mmol) at 0 °C, and the mixture was stirred for 45 min. NEt_3 (225 mg, 2.225 mmol) and **18** (95 mg, 0.445 mmol) were added, and the mixture was stirred at 65 °C for 15 min. The solvent was removed, and the residue was purified by preparative HPLC to give compound **41** (222 mg, 72%) as a yellow solid. UPLC retention time 1.13 min. ES/ESI 567 $[M + H]^+$.

11. A solution of **41** (222 mg, 0.323 mmol) in CH_2Cl_2 (2 mL), TFA (2 mL) and water (0.02 mL) was stirred at 25 °C for 0.5 h. Then, the mixture was kept for 16 h at 0 °C and for 1 h at 25 °C. The solvents were evaporated, and the residue was purified by preparative HPLC. The product was dissolved in CH_2Cl_2 and extracted with 1 N NaOH to give **11** (62 mg) as a yellow solid. UPLC retention time 0.59 min. ^{1}H NMR (400 MHz, CD_3OD): δ 7.59 (1H, d), 7.30 (1H, d), 7.18 (1H, d), 7.09 (1H, t), 6.58 (1H, d), 3.70 (1H, m), 3.20 (1H, m), 1.80−1.30 (8H, m). HR-MS $[M + H]^+$ calcd, 367.19893; found, 367.19910.

12 (HCl Salt). UPLC retention time 0.52 min. ^{1}H NMR (400 MHz, CD_3OD): δ 7.79 (1H, d),7.44 (1H, d), 7.41 (1H, d), 7.25 (1H, t), 6.64 (1H, d), 4.38 (1H, m), 3.70 (1H, m), 2.00−1.55 (8H, m). ES/ESI 367 $[M + H]^+$. HR-MS $[M + H]^+$ calcd, 367.19893; found, 367.19895.

45. A mixture of **42** (455 mg, 2.372 mmol), **23** (313 mg, 2.372 mmol), and NEt_3 (1392 mg, 13.76 mmol) in THF (30 mL) was stirred at 25 °C for 16 h. The solvent was removed, and the residue was extracted with ethyl acetate to give a gray solid (**43**), which was used without further purification in the next step. The solid was dissolved in DMF (7 mL), **44** (589 mg, 2.372 mmol) and NEt_3 (705 mg, 5.46 mmol) were added, and the mixture was heated for 3 h at 110 °C. Ethyl acetate was added, and the mixture was washed with water and brine. The organic phase was dried over Na_2SO_4, and the solvent was removed. The residue was purified by chromatography on silica (gradient cyclohexane/ethyl acetate) to give **45** (720 mg, 52%) as a light brown solid. UPLC retention time 1.01 min. ES/ESI 500 $[M + H]^+$.

13. A mixture of **45** (360 mg, 0.62 mmol) and 10% Pd/C (75 mg, 0.07 mmol) in methanol (20 mL) was stirred for 3.5 h at 25 °C in the presence of an atmosphere of H_2 (balloon). The mixture was filtered through Hyflo, the solvent was removed, and the residue was purified by preparative HPLC. Product containing fractions were combined and passed through an Isolute SCX-2 column to yield the free base of **13** (68 mg, 30%) as a yellow solid. UPLC retention time 0.59 min. ^{1}H NMR (400 MHz, CD_3OD): δ 7.59 (1H, d), 8.48 (1H, s), 7.46 (1H, d); 7.22 (1H, d), 7.14 (1H, d), 7.01 (1H, t), 6.48 (1H, d), 3.62 (1H, m), 2.77 (1H, m), 1.80−1.30 (8H, m). ES/ESI 366 $[M + H]^+$. HR-MS $[M + H]^+$ calcd, 366.20368; found, 366.20368.

Syk Kinase Assay. The assay was performed as end-point determination using 384-well microtiter plates. Compounds were tested as 8-point dose responses. The assays were prepared by addition of 50 nL of compound solution in 90% DMSO directly into the empty plate using a hummingbird dispenser (Zinsser, Germany). Subsequently, 4.5 μL of a mixture of 4 μM ATP and 4 μM peptide (5-Fluo-Ahx-GAPDYENLQELNKK-Amide) in reaction buffer (50 mM HEPES, pH 7.5, 1 mM DTT, 0.02% Tween-20, 0.02% BSA, 0.6% DMSO, 10 mM beta-glycerophosphate, 10 μM sodium orthovanadate, 1 mM $MgCl_2$, 3 mM $MnCl_2$) was added to each well. The kinase

DOI: 10.1021/jm5018863
J. Med. Chem. 2015, 58, 1950−1963

reactions were started by further addition of 4.5 μL of enzyme solution (4 nM Syk (2-635) in reaction buffer). After 60 min incubation at 30 °C, reactions were terminated by addition of 16 μL per well of EDTA stop solution. Product formation was measured in a microfluidic mobility shift assay (Caliper LC3000, PerkinElmer).

Syk Cellular Assay. Ramos B-cells were grown and passaged in RPMI 1640 medium (Gibco) containing 10% FCS. On the day of the experiment, cells were washed with serum-free medium and dispensed into microtiter plates followed by addition of compound and incubation for 30 min at 37 °C. The cells were then stimulated by addition of anti-IgM (Bioconcept, final concentration 20 μg/mL) for 15 min at 37 °C. In each experiment, 8-fold serial dilutions of compounds were tested. The stimulation was quenched by addition of 100 μL/well of formaldehyde (final conc. 2%) for 15 min, followed by centrifugation. The cell pellet was resuspended in 100 μL of 90% methanol and further incubated for 30 min at 4 °C. The cells were then washed three times with 2% FCS in PBS. Phospho-BLNK was assessed by flow cytometry using a FACSCalibur or a CyAn-(Hypercyt) instrument using anti-BLNK (pY84)Mab-Alexa647 (BD Bioscience). Fluorescence values were evaluated in FlowJo followed by Excel/XLfit. The IC_{50} values were calculated by using a factor taking into account the mean fluorescence intensity (MFI) of P-BLNK-stained activated Ramos cells and the percentage of stained cells above a threshold set to exclude >99% of unstained cells. The factor is calculated according to the formula F = MFI × percent positive cells.

Syk Assay in Human Blood. Blood was collected from healthy volunteers by venipuncture into Monovette heparin tubes. The whole blood was dispensed into microtiter plate wells, and compounds to be tested were added and incubated for 30 min at 37 °C. Into a second plate was added 10 μL of prewarmed anti-human CD32 (eBioscience, 10-fold concentrate; 50 μg/mL final). Then, 100 μL of blood + compound sample from the first plate was transferred to plate 2, mixed, and incubated for 5 min at 37 °C followed by red cell lysis in Lyse Fix (BD Bioscience). The plate was then centrifuged, and the cell pellet was permeabilized in 90% methanol and washed as described above. The cells were stained with anti-CD14-Pacific Blue (eBioscience) to identify the monocytes and anti-SLP76 (pY128)-mAb-Alexa647 (BD Bioscience). The IC_{50} values for inhibition of P-SLP76 in $CD14^+$ monocytes was assessed by flow cytometry as described above.

Mouse Bone Marrow Cell Proliferation Assay. Serial dilutions of compound samples were prepared in 50 μL of RPMI medium in a 96-well plate. Freshly isolated bone marrow cells from C57BL/6 mice were adjusted to 5×10^5/mL in RPMI containing WEHI and L929 conditioned medium (as a source of IL-3) or recombinant IL-3 at appropriate concentrations. Fifty microliters of the cell suspension (2.5×10^4 cells) was added to each well containing compounds. Cultures without any compound sample were used as high controls; cultures without compound or IL-3 were used as low controls. Cultures were incubated for 4 days at 37 °C in 5% CO_2. One microcurie of ^{3}H-thymidine was added to each well and incubated for an additional 5 h. Cells were then harvested with a Betaplate 96-well harvester on filter paper, and the filter was washed, dried, and counted after addition of scintillation liquid in a Betaplate counter.

Zap70 Cellular Assay. Jurkat T-cells were washed twice with RPMI 1640/0.1% FCS and resuspended in the same medium. Compounds to be tested were dispended into wells of a microtiter plate (25 μL of compound solution 2-fold concentrated in RPMI + 0.1% FCS). Cells were added to the wells with compound (2×10^5 cells/25 μL) and incubated for 30 min at 37 °C. Stimulation of the TCR was achieved by addition of 50 μL/well of anti-TCR antibody OKT3 (ACE10273, 30 μg/mL final concentration) diluted in prewarmed medium and incubated for 2 min at 37 °C. The stimulation was stopped by addition of 100 μL of PFA/PBS (2% PFA final concentration) followed by incubation for 15 min at 37 °C. Cells were centrifuged and resuspended in 100 μL of 90% methanol and further incubated for 30 min at 4 °C. Permeabilized cells were washed once with PBS and then twice with 150 μL/well FACS buffer (PBS + 2% FCS), and the last cell pellet was stained with anti-SLP76(pY128)mAb-Alexa647 (BD Bioscience) for 80 min at RT in the dark, washed, resuspended in 200 μL of FACS buffer, and read on a FACS Calibur instrument. The IC_{50} values were calculated based on the factor as described above for Ramos B cells.

Collagen-Induced Arthritis and Histology. Female Lewis rats (140−160g) were purchased from Janvier. Rats were kept under standard conditions (optimal health conditions [CHC], 22 °C in special, acclimatized animal rooms with 12 h dark−light cycles, with light from 0600 to 1800) with free access to tap water and pelleted rodent chow. The rats were allowed to acclimatize upon arrival for at least 7 days before entering the study. This study was performed according to current Swiss animal protection laws issued by the Cantonal Veterinary Office Basel-Stadt, Switzerland. Freund's incomplete adjuvant (IFA, Difco, Detroit, MI) was mixed with porcine collagen type II (Chondrex, Redmond, WA) using a polytron on ice. The final solution consisted of 200 μg of collagen in 200 μL of IFA. Two hundred microliters of this was injected intradermally (i.d.) into the base of the tail of an isofluorane-narcotisized rat. After 7 days, the animal was boosted i.d. with a fresh batch of the immunization solution (this time, 100 μg in 100 μL) in an adjacent site at the base of the tail. When sufficient animals had developed arthritis, they were randomized into groups of 6 or 7 so that they all had the same average swelling score. This was on day 15 after initial immunization. At this time, 300 μL of heparinized blood was taken for baseline PD assessment. Compound was diluted in 0.5% CMC/0.5% Tween-80 in water and was applied p.o. at a dose of 3, 10, and 30 mg/kg q.d. Compound was applied in a therapeutic setting starting at day 15 and continued until day 28. Swelling was scored three times a week. On days 19 and 20, 300 μL of heparinized blood was taken at trough (24 h) and at 4 h (peak) for PD, and 100 μL of EDTA blood taken at 4, 8, and 24 h for PK analysis. On day 28, animals were sacrificed, and hind paws were taken for histopathological analysis. Animals were weighed regularly throughout the study. Mean values of each group were calculated. Scoring of the hind paw swelling was done on a composite scale of 0−12 per rat, evaluating each paw by visual inspection in the metatarsal region with score 0−3 and in the ankle with score 0−3, thus obtaining a maximal score of 6 per paw. The paw scores were summed to obtain a score for each individual animal. The individual sum scores of all animals were averaged, and SEMs were calculated. The scoring system used was as follows: 0, no detectable sign of inflammation; 1, light swollen region; 2, more obviously swollen region; 3, ankylosis or severely swollen region. Hind paws samples were fixed in 10% buffered formalin for 48 h, decalcified over 16 days in Immunocal (Decal Chemical Corp., Tallman, NY) changed every 3−4 days, processed, and embedded in paraffin (paraplast tissue embedding medium; Leica Microsystems, Buffalo Grove, IL). Three-micrometer thick sections were stained with Giemsa and safranin O. Histopathological changes were blindly scored on a scale of 0 (normal) to 3 (severe changes). The following parameters were assessed: inflammatory cell infiltrates, joint damage, and proteoglycan loss. Statistical analysis for paw swelling, body weight, and histopathological assessment were performed with a Dunnet's multiple comparisons test (one-way ANOVA).

Incubation of 11 with Monkey Liver Slices. Animal experiments were performed in accordance with Swiss Animal Welfare regulations. Freshly excised liver was collected from an animal after euthanasia. All tissue slice experiments were carried out using Williams medium E supplemented with fetal bovine serum (10%), glucose (27 mM), insulin (1 μM), hydrocortisone (100 μM), methionine (500 μM), gentamycin (100 μM), and amphotericin B (3 μM). Stock solutions of test compounds (2 mM) were prepared in DMSO. Tissue cores (8 mm) from freshly excised liver were prepared using a tissue-coring tool. Slices of 230 μm thickness were prepared from the cores using a MD6000 Krumdieck live tissue microtome (Alabama Research and Development, Munford, AL), filled with ice-cold medium under bubbling of O_2 and CO_2. After preparation, slices were washed and kept on ice in medium until use. Liver slices (4 per incubation vessel) were preincubated for 1 h at 37 °C in 2 mL of medium under an atmosphere of 75% O_2, 5% CO_2, 20% N_2 at 98% humidity in a rotating culture (4 rotations/min) in a HERAcell 240i incubator (Thermo Fischer Scientific, Waltham, MA). Subsequently, the test compound

DOI: 10.1021/jm5018863
J. Med. Chem. 2015, 58, 1950−1963

(10 or 20 μM) was added, and the slices were incubated for a further 8 or 18 h. At the end of the incubation time, each incubation sample was quenched with 2 mL of cold acetonitrile (4 °C), and the mixture was frozen at −80 °C until workup.

■ ASSOCIATED CONTENT

Accession Codes

The coordinates for the structures of **1**, **10**, and **11** bound to the kinase domain of Syk have been deposited in the RCSB Protein Data Bank under PDB IDs 4RX9, 4RX7, and 4RX8, respectively.

■ AUTHOR INFORMATION

Corresponding Author

*Tel: +41 61 3243342. Fax: +41 61 3246735. E-mail: gebhard.thoma@novartis.com.

Notes

The authors declare no competing financial interest.

■ ACKNOWLEDGMENTS

We gratefully acknowledge the expert assistance of Valerie Caballero, Thierry Délémonté, Ralf Endres, Werner Gertsch, Stephanie Harlfinger, Alice Hauchard, Dorothee Lehmann, Alexandre Luneau, Jürg Peter, Marc Schäfer, Tanja Senn, Phuoc Thanh Thai, and Grazyna Wieczorek.

■ ABBREVIATIONS USED

BCR, B-cell receptor; BLNK, B-cell linker protein; CDI, carbonyldiimidazole; COMU, (1-cyano-2-ethoxy-2-oxoethylidenaminooxy)dimethylamino-morpholino-carbenium hexafluorophosphate; DIPEA, *N*,*N*-diisopropylethylamine; DMAP, 4-dimethylaminopyridine; DMF, dimethylformamide; GLP, good laboratory practice; hERG, human *ether-à-go-go* related gene; ITAM, immunotyrosine activating motif; LiHMDS, lithium hexamethyldisilazide; MAPK, mitogen-activated protein kinase; *m*-CPBA, *meta*-chloroperoxybenzoic acid; NMP, *N*-methyl-2-pyrrolidone; NFκB, nuclear factor kappa-light-chain-enhancer of activated B-cells; PI3-kinase, phosphoinositide-3 kinase; PK, pharmacokinetics; PKC, protein kinase C; PLCγ2a, phospholipase C-γ2a; SH2, Src 2; SEM, standard error of the mean; SLP65, Src homology 2 domain-containing leukocyte-specific phosphoprotein of 65 kDa; SLP76, SH2 domain containing leukocyte protein of 76 kDa; Syk, spleen tyrosine kinase; TFA, trifluoroacetic acid; UPLC, ultra-performance liquid chromatography; Xantphos, 4,5-bis(diphenylphosphino)-9,9-dimethylxanthene; ZAP70, zeta-chain-associated protein kinase

■ REFERENCES

(1) (a) Mócsai, A.; Ruland, J.; Tybulewicz, V. L. J. The SYK tyrosine kinase: a crucial player in diverse biological functions. *Nat. Rev. Immunol.* **2010**, *10*, 387−402. (b) Kulathu, Y.; Grothe, G.; Reth, M. Autoinhibition and adapter function of Syk. *Immunol. Rev.* **2009**, *232*, 286−299. (c) Gilfillan, A. M.; Rivera, J. The tyrosine kinase network regulating mast cell activation. *Immunol. Rev.* **2009**, *228*, 149−169. (d) Geahlen, R. L. Syk and pTyr'd: signaling through the B cell antigen receptor. *Biochim. Biophys. Acta* **2009**, *1793*, 1115−1127. (e) Koretzky, G. A.; Abtahian, F.; Silverman, M. A. *Nat. Rev. Immunol.* **2006**, *6*, 67−78.

(2) (a) Bajpai, M.; Chopra, P.; Dastidar, S. G.; Ray, A. Spleen tyrosine kinase: a novel target for therapeutic intervention of rheumatoid. *Expert Opin. Invest. Drugs* **2008**, *17*, 641−659. (b) Siraganian, R. P.; Zhang, J.; Suzuki, K.; Sada, K. Protein tyrosine kinase Syk in mast cell signaling. *Mol. Immunol.* **2002**, *38*, 1229−1233. (c) Wong, B. R.; Grossbard, E. B.; Payan, D. G.; Masuda, E. S. Targeting Syk as a treatment for allergic and autoimmune disorders. *Expert Opin. Invest. Drugs* **2004**, *13*, 743−763. (d) Ghosh, D.; Tsokos, G. C. Spleen tyrosine kinase: an Src family of non-receptor kinase has multiple functions and represents a valuable therapeutic target in the treatment of autoimmune and inflammatory diseases. *Autoimmunity* **2010**, *43*, 48−55.

(3) Geahlen, R. L. Getting Syk: spleen tyrosine kinase as a therapeutic target. *Trends Pharmacol. Sci.* **2014**, *35*, 414−422.

(4) Taniguchi, T.; Kobayashi, T.; Kondo, J.; Kazuhiro, T.; Nakamura, H.; Suzuki, J.; Nagai, K.; Yamada, T.; Nakamura, S.; Yamamura, H. Molecular cloning of a porcine gene syk that encodes a 72-kDa protein-tyrosine kinase showing high susceptibility to proteolysis. *J. Biol. Chem.* **1991**, *266*, 15790−15796.

(5) (a) Singh, R.; Masuda, E. S.; Payan, D. G. Discovery and development of spleen tyrosine kinase (Syk) inhibitors. *J. Med. Chem.* **2012**, *55*, 3614−3643. (b) Moore, W. J.; Richard, D.; Thorarensen, A. An analysis of the diaminopyrimidine patent estates describing spleen tyrosine kinase inhibitors by Rigel and Portola. *Expert Opin. Ther. Patents* **2010**, *20*, 1703. (c) Norman, P. Spleen tyrosine kinase inhibitors: a review of the patent literature 2010−2013. *Expert Opin. Ther. Patents* **2014**, *24*, 573−595. (d) Castillo, M.; Forns, P.; Erra, M.; Mir, M.; Lopez, M.; Maldonado, M.; Orellana, A.; Carreno, C.; Ramis, I.; Miralpeix, M.; Vidal, B. Highly potent aminopyridines as Syk kinase inhibitors. *Bioorg. Med. Chem. Lett.* **2012**, *22*, 5419−5423. (e) Forns, P.; Esteve, C.; Taboada, L.; Alonso, J. A.; Orellana, A.; Maldonado, M.; Carreno, C.; Ramis, I.; Lopez, M.; Miralpeix, M.; Vidal, B. Pyrazine-based Syk kinase inhibitors. *Bioorg. Med. Chem. Lett.* **2012**, *22*, 2784−2788. (f) Lucas, M. C.; Goldstein, D. M.; Hermann, J. C.; Kuglstatter, A.; Liu, W.; Luk, K. C.; Padilla, F.; Slade, M.; Villasenor, A. G.; Wanner, J.; Xie, W.; Zhang, X.; Liao, C. Rational design of highly selective spleen tyrosine kinase inhibitors. *J. Med. Chem.* **2012**, *55*, 10414−10423. (g) Padilla, F.; Bhagirath, N.; Chen, S.; Chiao, E.; Goldstein, D. M.; Hermann, J. C.; Hsu, J.; Kennedy-Smith, J. J.; Kuglstatter, A.; Liao, C.; Liu, W.; Lowrie, L. E., Jr.; Luk, K. C.; Lynch, S. M.; Menke, J.; Niu, L.; Owens, T. D.; O-Yang, C.; Railkar, A.; Schoenfeld, R. C.; Slade, M.; Steiner, S.; Tan, Y.-C.; Villasenor, A. G.; Wang, C.; Wanner, J.; Xie, W.; Xu, D.; Zhang, X.; Zhou, M.; Lucas, M. C. Pyrrolopyrazines as selective spleen tyrosine kinase inhibitors. *J. Med. Chem.* **2013**, *56*, 1677−1692. (h) Lucas, M. C.; Bhagirath, N.; Chiao, E.; Goldstein, D. M.; Hermann, J.; Hsu, P.-Y.; Kirchner, S.; Kennedy-Smith, J.; Kuglstatter, A.; Lukacs, C.; Menke, J.; Niu, L.; Padilla, F.; Peng, Y.; Polonchuk, L.; Railkar, A.; Slade, M.; Soth, M.; Xu, D.; Yadava, P.; Yee, C.; Zhou, M.; Liao, C. Using ovality to predict non-mutagenic, orally efficacious pyridazine amides as cell specific spleen tyrosine kinase inhibitors. *J. Med. Chem.* **2014**, *57*, 2683−2691. (i) Liddle, J.; Atkinson, F. L.; Barker, M. D.; Carter, P. S.; Curtis, N. R.; Davis, R. P.; Douault, C.; Dickson, M. C.; Elwes, D.; Garton, N. S.; Gray, M.; Hayhow, T. G.; Hobbs, C. I.; Jones, E.; Leach, S.; Leavens, K.; Lewis, H. D.; McCleary, S.; Neu, M.; Patel, V. K.; Preston, A. G. S.; Ramirez-Molina, C.; Shipley, T. J.; Skone, P. A.; Smithers, N.; Somers, D. O.; Walker, A. L.; Watson, R. J.; Weingarten, G. G. Discovery of GSK143, a highly potent, selective and orally efficacious spleen tyrosine kinase inhibitor. *Bioorg. Med. Chem. Lett.* **2011**, *21*, 6188−6194. (j) Moy, L. Y.; Jia, Y.; Caniga, M.; Lieber, G.; Gil, M.; Fernandez, X.; Sirkowski, E.; Miller, R.; Alexander, J. P.; Lee, H.-H.; Shin, J. D.; Ellis, J. M.; Chen, H.; Wilhelm, A.; Yu, H.; Vincent, S.; Chapman, R. W.; Kelly, N.; Hickey, E.; Abraham, W. M.; Northrup, A.; Miller, T.; Houshyar, H.; Crackower, M. A. Inhibition of spleen tyrosine kinase attenuates allergen-mediated airway constriction. *Am. J. Respir. Cell Mol. Biol.* **2013**, *49*, 1085. (k) Luca, M. C.; Tan, S.-L. Small-molecule inhibitors of spleen tyrosine kinase as therapeutic agents for immune disorders: will promise meet expectations? *Future Med. Chem.* **2014**, *6*, 1811−1827.

(6) Coffey, G.; DeGuzman, F.; Inagaki, M.; Pak, Y.; Delaney, S. M.; Ives, D.; Betz, A.; Jia, Z. J.; Pandey, A.; Baker, D.; Hollenbach, S. J.; Phillips, D. R.; Uma Sinha, U. Specific inhibition of spleen tyrosine kinase suppresses leukocyte immune function and inflammation in

DOI: 10.1021/jm5018863
J. Med. Chem. 2015, 58, 1950−1963

animal models of rheumatoid arthritis. *J. Pharmacol. Exp. Ther.* **2012**, *340*, 350−359.
(7) *BIIB057 in Subjects with Rheumatoid Arthritis and Inadequate Response to Disease-Modifying Antirheumatic Drugs (EMBRACE)*; ClincalTrials.gov; http://www.clinicaltrials.gov/ct2/show/NCT01652937?term=biib-057&rank=1.
(8) (a) Golden, A. P.; Li, N.; Chen, Q.; Lee, T.; Nevill, T.; Cao, X.; Johnson, J.; Erdemli, G.; Ionescu-Zanetti, C.; Urban, L.; Holmqvist, M. IonFlux: a microfluidic patch clamp system evaluated with human ether-a-go-go related gene channel physiology and pharmacology. *Assay Drug Dev. Technol.* **2011**, *9*, 608−619.
(9) *The Non-clinical Evaluation of the Potential for Delayed Ventricular Repolarization (QT Interval Prolongation) by Human Pharmaceuticals*, ICH S7B; International Conference on Harmonisation of Technical Requirements for Registration of Pharmaceuticals for Human Use, 2005. http://www.ich.org/fileadmin/Public_Web_Site/ICH_Products/Guidelines/Safety/S7B/Step4/S7B_Guideline.pdf.
(10) Currie, K. S.; Kropf, J. E.; Lee, T.; Blomgren, P.; Xu, J.; Zhao, Z.; Gallion, S.; Whitney, J. A.; Maclin, D.; Lansdon, E. B.; Maciejewski, P.; Rossi, A. M.; Rong, H.; Macaluso, J.; Barbosa, J.; Di Paolo, J. A.; Mitchell, S. A. Discovery of GS-9973, a selective and orally efficacious inhibitor of spleen tyrosine kinase. *J. Med. Chem.* **2014**, *57*, 3856−3873.
(11) Thoma, G.; Blanz, J.; Buhlmayer, P.; Druckes, P.; Kittelmann, M.; Smith, A. B.; van Eis, M.; Vangrevelinghe, E.; Zerwes, H.-G.; Che, J.; He, X.; Jin, Y.; Lee, C. C.; Michellys, P.-Y.; Uno, T.; Liu, H. Syk inhibitors with high potency in presence of blood. *Bioorg. Med. Chem. Lett.* **2014**, *24*, 2278−2282.
(12) Jaguar software was used for DFT/B3LYP calculations in gas phase with the 6-311++G** basis set. Jaguar is a high- performance *ab initio* package for both gas- and solution-phase simulations. Bochevarov, A. D.; Harder, E.; Hughes, T. F.; Greenwood, J. R.; Braden, D. A.; Philipp, D. M.; Rinaldo, D.; Halls, M. D.; Zhang, J.; Friesner, R. A. Jaguar: a high-performance quantum chemistry software program with strengths in life and materials sciences. *Int. J. Quantum Chem.* **2013**, *113*, 2110−2142.
(13) It is worth mentioning that the pyrimidine analogue of **12** also showed a very limited oral bioavailability of 4%.
(14) Compound **11** was assessed in the KINOMEscan screening platform, which employs an active site-directed competition binding assay to quantitatively measure interactions between test compounds and kinases. These assays do not require ATP and thereby report thermodynamic interaction affinities, as opposed to IC_{50} values, which can depend on the ATP concentration. See http://www.discoverx.com/services/drug-discovery-development-services/kinase-profiling/kinomescan.
(15) Williams, R. O. Collagen-induced arthritis as a model for rheumatoid arthritis. *Methods Mol. Med.* **2004**, *98*, 207−216.

DOI: 10.1021/jm5018863
J. Med. Chem. 2015, 58, 1950−1963